

Optimal Configuration of Finned Annular Sector Duct Filled With Porous Media

by

Hafsa Hareem



A thesis

Submitted for the Degree of Master of Science

in

Mathematics

Supervised by


Dr. Mazhar Iqbal

School of Natural Sciences,
National University of Sciences and Technology,
H-12, Islamabad, Pakistan

© Hafsa Hareem, March 2018

National University of Sciences & Technology**MASTER'S THESIS WORK**

We hereby recommend that the dissertation prepared under our supervision by: Ms. Hafsa Hareem, Regn No. 00000117244 Titled: Optimal Configuration of Finned Annular Sector Duct Filled With Porous Media be accepted in partial fulfillment of the requirements for the award of **MS** degree.

Examination Committee Members1. Name: Dr. Meraj Mustafa HashmiSignature: 2. Name: Dr. Mujeeb ur RehmanSignature: 

3. Name: _____

Signature: _____

4. External Examiner: Dr. Masood KhanSignature: Supervisor's Name: Dr. Mazhar IqbalSignature: 


Head of Department

14-03-18
Date

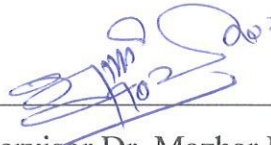
COUNTERSIGNEDDate: 14-03-18


Dean/Principal

THESIS ACCEPTANCE CERTIFICATE

Certified that final copy of MS thesis written by Ms. Hafsa Hareem, (Registration No. 00000117244), of School of Natural Sciences has been vetted by undersigned, found complete in all respects as per NUST statutes/regulations, is free of plagiarism, errors, and mistakes and is accepted as partial fulfillment for award of MS/M.Phil degree. It is further certified that necessary amendments as pointed out by GEC members and external examiner of the scholar have also been incorporated in the said thesis.

Signature: _____



Name of Supervisor Dr. Mazhar Iqbal

Date: _____

14-03-2018

Signature (HoD): _____



Date: _____

14-03-18

Signature (Dean/Principal): _____



Date: _____

14-03-18

Dedicated
to
My Parents

Acknowledgment

I am very appreciative of Allah Almighty with regards to His direction and support all through this thesis. I am obliged to my parents and faculty. I appreciate my mother and father for raising and enlightening me through their utmost efforts and for guiding me on the right path. I am appreciative for the pick and drop services that my little brother provided in the span of my thesis and my sister for patiently listening to all my problems. Most of the credit goes to my supervisor Dr. Mazhar Iqbal for his consistent support and I am thankful to him for driving me to deliver my best. Last but not the least, I want to mention my colleagues and peers without whom i could not have done this.

Abstract

In the current study, optimal configurations for finned annulus, filled with porous media, have been investigated to maximize the convective heat transfer and minimize the friction effect subject to constant heat flux boundary conditions. Genetic algorithm (GA) has been employed to find out the optimal geometry out of vast choices of geometrical parameters; ratio of radii of the inner to outer pipe and sector angle of channel. Finite difference method (FDM) is applied to compute the governing mathematical model. Chilton-Colburn j factor is employed as the objective function and numerical solutions of the momentum and energy equations are used as function values to the optimizer. The results indicate that for a fixed Prandtl number (Pr) the optimal geometry transforms with the variation in permeability of the porous media which is in line with the physics of the problem. This thesis interpolates material from the paper submitted by the author [1].

Contents

- 1 Introduction and Literature Review 1**
 - 1.1 Introduction 1
 - 1.2 Literature Review 2
 - 1.3 Preliminaries 7
 - 1.3.1 Fluid Flow 7
 - 1.3.2 Mathematical Models Governing Fluid Flow 10
 - 1.3.3 Heat Transfer 12
 - 1.3.4 Modes of Heat Transfer 12
 - 1.3.5 Bulk mean temperature 14
 - 1.3.6 Generalized Energy Equation 14
 - 1.3.7 Fluid Flow and Heat Transfer Parameters 15
 - 1.3.8 Boundary Conditions 18
 - 1.3.9 Boundary Layers 19

- 2 Solution Strategies 21**
 - 2.1 Introduction 21
 - 2.2 Problem Formulation 21
 - 2.3 Discretization 27
 - 2.4 Numerical Technique 28
 - 2.5 Validation of Results 28
 - 2.6 Optimization Methods 29

<i>CONTENTS</i>	VI
2.6.1 Genetic Algorithm	33
2.6.2 GA and TRM : A Comparison	35
3 Optimal Configuration of an Annular Sector Duct	38
3.1 Introduction	38
3.2 Optimization Problem	38
3.2.1 Modeling of Genetic Algorithm	40
3.3 Results and Discussion	42
4 Conclusions and Further work	52
4.1 Conclusions	52
4.2 Further extensions	53
References	54

List of Figures

2.1	Geometry of duct	22
2.2	(a):GA-best fitness and best individual plot (b):TRM-current point and function value plot	37
3.1	Values of fRe for various \tilde{R}	41
3.2	Values of Nu for for various \tilde{R}	41
3.3	Best fitness plot at $Pr=0.707$ for (a): $\hat{K} = 0.001$ (b): $\hat{K} = 0.01$ (c): $\hat{K} =$ 0.1 (d): $\hat{K} = 1$ (e): $\hat{K} = 10$ (f): $\hat{K} = 100$	45
3.4	Range plot at $Pr= 0.707$ when (a): $\hat{K} = 0.001$ (b): $\hat{K} = 0.01$ (c): $\hat{K} = 0.1$ (d): $\hat{K} = 1$ (e): $\hat{K} = 10$ (f): $\hat{K} = 100$	46
3.5	Velocity profile at $Pr=0.707$ for (a): $\hat{K} = 100$ (b): $\hat{K} = 10$ (c): $\hat{K} = 1$ (d): $\hat{K} = 0.1$ (e): $\hat{K} = 0.01$ (f): $\hat{K} = 0.001$	50
3.6	Temperature profile at $Pr=0.707$ for (a): $\hat{K} = 100$ (b): $\hat{K} = 10$ (c): $\hat{K} = 1$ (d): $\hat{K} = 0.1$ (e): $\hat{K} = 0.01$ (f): $\hat{K} = 0.001$	51

Chapter 1

Introduction and Literature Review

1.1 Introduction

Optimization is an emerging technique in the sphere of Computational Fluid Dynamics (CFD) for finding the best results for numerical simulation in the various disciplines of applied sciences and engineering problems affiliated with fluid flow and heat transfer phenomena. It is a technique employed to find the best possible solution to a problem. In the field of applied sciences and engineering, optimization usually leads to the search of a point where the value of objective function is at its minimum or maximum. It is more effective and efficient method in the right direction after denying the old hit and trial methods. It has helped reduce cost and effort and save time, for the expensive experiments held for construction and maturation of fresh products.

There are a variety of methods available for the optimization of ones problem which can be easily executed on a computer. Optimization can be categorized into uni-disciplinary and multi-disciplinary based on the kind of results that are needed. Optimization techniques that are uni-disciplinary are divided into gradient based algorithms, evolutionary algorithms, simulated annealing algorithms and hybrid algorithms. Whereas multi-

disciplinary optimization techniques characterized into Collaborative Optimization (CO), Concurrent Subspace Optimization (CSSO), Bi-Level Integrated System Synthesis (BLISS) and Analytical Target Cascading (ATC). When restraints are applied on the objective function of optimization, it is termed as constrained optimization otherwise it is unconstrained optimization.

Surface elongation and extension has been a significant technique used to increase the heat transfer rate between fundamental surfaces and the medium surrounding it. Fins are the most popular extended surfaces widely used in the fields of petroleum manufacturing, electronics, chemical factory, power plants, nuclear processes, aerodynamics etc. Fins can be adjoined inside or outside a pipe or between two concentric pipes for the amplification of heat transfer rate. Although fins are quite useful in increasing heat transfer rate as they provide more surface area for heat transfer however they possess a few drawbacks of increasing friction, weight, cost etc. Hence optimization of duct and fin configuration has become an intriguing sphere of study. By optimizing the radius of concentric pipes and number of fins used, we can raise the heat transfer rate and decrease the friction effect. Hence optimization of duct and fin configuration has become an intriguing sphere of study. In the current research, we have optimized the radius of concentric pipes and number of fins used to raise the heat transfer rate and drop the friction effect for two concentric pipes which have longitudinal fins joined within the annulus between the internal and external pipe.

Some elementary definitions and fundamental concepts are included in this chapter. Also a detailed literature review has been carried out of the problem solved in succeeding chapters.

1.2 Literature Review

Fluid flow and heat transfer have always been an area of interest for scientists. F. Liu [2] studied that duct geometry has great impact on bifurcation structures, heat transfer

enhancement potential and flow stability of forced convection. It is concluded that when friction of flow experiences a minor boost, a noteworthy raise in heat transfer potential is observed. This can be achieved by rearranging the flow from one branch to another. I. Kurtbas and N. Celik. [3] experimentally investigated mixed convection heat transfer of a fluid flowing through a horizontal rectangular channel. Open-cell metal foams of different porosities are placed in the channel. Average and local Nusselt numbers were calculated as the functions of Reynolds and Richardson numbers. It was concluded that the average Nusselt number experiences a rapid upsurge that is proportional to the pore density and the local Nusselt number rises quickly regarding a analyst value of Reynolds number.

K. Hooman et al. [4] analyzed the properties of first and second law of thermodynamics for fully developed convective transfer of heat within a porous saturated duct having a rectangular cross section. Three different thermal boundary conditions were imposed under which analytical results for Nusselt number and temperature distribution were given. It was concluded that heat transfer rate is best, when porous media shape parameter is less than 10 and the sides of the duct along the width are heated while others are insulated. Whereas when porous media shape parameter is greater than 10, the best results are obtained when only one side of duct is insulated.

M. R. H. Nobari and M. T. Mehrabani [5] numerically discussed flow and heat transfer carried out in curved shaped eccentric annuli. This study investigates the influence of Dean Number, curvature of annulus, eccentricity and Prandth number on fluid flow field and thermal traits, when thermal boundary conditions are altered. It is observed that when dean number is large, rate of heat transfer can be escalated for curved eccentric annuli. This contrasts with straight annuli behavior .The amplification of rate of heat transfer in eccentric curved annuli, for large dean number relies on curvature ratio and eccentricity of annulus. Z. Y. Li et al. [6] employed mixing length theory on annular sector ducts to simulate a flow that is fully developed and turbulent in nature. Five apex angles along and four radius ratios with the Reynolds number ranging in 104 - 105 are considered in this research. The study showed that the friction factor, gathered from the turbulence

models does not coincide with test data and mixing length theory is best suited for heat transfer through fully developed flow.

E. H. Zaim and S. A. G. Nassab [7] numerically analyzed convective heat transfer through water. For this research supercritical pressure is being applied on water flowing through a narrow annulus. Inlet fluid temperature governs the Nusselt number and when the temperature advances to pseudo-critical level Nusselt number escalates. O. Zeitoun and A. S. Hegazy [8] numerically investigated the heat transfer rate for laminar flow through pipes with fins of different height attached in it. The wall temperature is spread uniformly. It was concluded that when pipes are taken to be internally finned then fin height has a great impact on the flow and heat transfer characteristics. M. J. Lin et al. [9] numerically studied developing laminar flow and heat transfer in annular sector ducts. It was concluded that both entrance lengths, hydrodynamic and thermal, experience a decrease when the sector angle along with the ratio of diameters of inner and outer pipe expand. Also the development of hydrodynamic boundary layer falls short to that of thermal boundary layer. I. K. Adegun et al. [10] numerically analyzed forced convection heat transfer in finned elliptical ducts and the influence that Reynolds number, Prandtl number, aspect ratio, fin heights, number of fins and orientations of the duct has on the heat transfer coefficient, history of temperature and velocity vector. They employed Finite Difference Method (FDM) to uncover the solution. Results show that eight fins optimize heat transfer. Nusselt number, average velocity and bulk fluid temperature are improved when inclination angle is between 0° and 75° . For $50 \leq Reynoldsnumber \leq 200$ the inclinations do not have a significant effect on heat transfer rate but when the value of Reynolds number exceeds the critical 200, the influence of inclination is more noticeable. M. Kaviany [11] studied laminar fluid flow in a porous media contained between two parallel plates. The plates are kept at a constant and equal pressure. The study concluded that in case of a fully developed field, the Nusselt number increases with the rise in shape parameter of porous media. The excess pressure drop has opposite effect than the effect of Nusselt number, it decreases with the increase in the value of shape parameter.

Muhammad Ishaq et al. [12] studied laminar forced convective heat transfer when the flow is assumed to be fully developed and the fluid is moving through a finned double pipe annulus. The fins are taken to be triangular with alternating heights. Simulations are carried out under the boundary condition of constant heat transfer rate per unit axial length applied on the heat transferring surfaces. Different height fins are employed in two groups and their influence on heat transfer in finned ducts is determined, along with the configuration of annulus. Discontinuous Galerkin Finite Element Method (DG-FEM) is adapted to solve the governing equations. Friction factor, Nusselt number and Colburn's j factor are investigated for numerous geometries. It was observed that when fins of various heights are activated in two groups, the flow and thermal attributes can be improved by adjusting the velocity and temperature distribution. O. Cekmer et al. [13] studied laminar, fully developed forced convection heat transfer through a parallel plate channel. The problem was modeled with the help of asymmetric uniform heat flux boundary conditions. The results showed that the variation in the overall Nusselt number is continuous for all considered values of the Darcy number, and it does not depend on the heat flux ratio. H. J. Sung et al. [14] numerically analyzed forced convection heat transfer and fluid flow through a channel which is partially filled with porous media. Governing equations are solved by employing Brinkman- Forchheimer extended Darcy model for porous media. The results indicate that as the thickness of porous substrate increases or Darcy number decreases, the rate of fluid flow experiences an upsurge. While keeping the Darcy number constant, when the ratio of thermal conductivities increase, the heat transfer rate experiences an upsurge. The practicality of using porous media to increase heat transfer is also analyzed. It was found that thicker and denser porous media is not suitable, while considering pressure drop in electrical cooling equipment.

Optimization of heat transfer in a double tube with fins attached in it was carried out by S. Colle and C. R. Maliska [15] where the flow was considered to be laminar. They also formed an association between the Reynolds number, friction factor, height, fin radius and the number of fins. Genetic algorithm was used for the optimization of

fin configuration carried out by G. Fabbri [16] where the temperature is distributed in two dimensions. The study was conducted to investigate the fin thickness for which fin effectiveness is maximum. Z. Iqbal et al. [17] conferred on the optimization of fin shape adhered with the exterior of an inner pipe about a double pipe geometry. The research concludes that PCHIP yields the optimal fin shape. The optimization of fin shape is highly reliant on the ratio of radii, number of fins, control points and characteristic length. All these parameters establish the fin profile to be triangular or wavy (one or more crest) for equivalent diameter and the fin profile can be parabolic and wavy for hydraulic diameter. Trapezoidal, parabolic and triangular fins can be used to bring about 312% improvement in Nusselt number. Z. Iqbal et al. [18] took up the optimization of a double pipe with trapezoidal fins attached with the inner pipe. Genetic algorithm and trust region methods are employed for the optimization of finned annulus. The maximum optimal value of Nusselt number has tremendous inclination upon the measurement of internal pipe. The optimum number of fins is directly proportional to the radius of inner pipe. When fins are abundant in number the optimum value can be actualized for higher fins. The dependence of Nusselt number on measure of internal pipe amplifies with the amount of fins employed. Genetic algorithm is more expensive than Trust Region method but it gives more reliable results and converges to global optimum. Z. Iqbal et al. [19] optimized an annulus with parabolic fins for convective heat transfer rate. Genetic algorithm and Trust Region method have been employed as the optimization techniques. The optimal configuration relies on both the hydraulic and equivalent diameter. When parabolic fins are compared with triangular and trapezoidal fins, its optimal configuration indicates that no fin shape is perfect according to every criteria. Z. Iqbal et al. [20] optimized the configuration of longitudinal fins adhered to the outer surface of the inner pipe in concentric pipe geometry. The researchers maximized the conjugate heat transfer coefficient by employing genetic algorithm. It is concluded that the optimal fin shape is dependent on the number of fins and their characteristic length, conduction properties of the heated surfaces and number of control points. The optimal fin shape that maximizes the conjugate heat

transfer coefficient is wavy and the optimal fin configuration improves the Nusselt number till 289%. M. Iqbal and H. Afaq [21] numerically analyzed fluid flow and heat transfer through an annular sector duct filled with porous media which indicated that an optimum geometry exists where we can observe heat transfer rate at its peak. Also as far as we know no research has been conducted to find the optimum value of fluid flow and heat transfer through porous media filled inside an annular sector duct. Hence my research work is motivated by this topic.

1.3 Preliminaries

In this section we will consider some basic concepts concerning our study, along with some useful dimensionless quantities.

1.3.1 Fluid Flow

Fluid

A fluid can be defined as “a substance that deforms continuously when acted on by a shearing stress of any magnitude”. Fluids take the shape of the container and they have the ability to flow [22].

Steady and Unsteady Flow

All the characteristics of a steady state flow are taken as independent of time. It can be mathematically represented as

$$\frac{\partial \phi}{\partial t} = 0 \tag{1.1}$$

where ϕ is any property of the fluid like velocity, density etc and $\frac{\partial}{\partial t}$ is partial derivative with respect to time. If a fluid flow does not satisfy the above property it is called unsteady or transient flow [22].

Laminar and Turbulent Flow

If the Reynolds number of fluid is less than 2100 than the flow is considered to be laminar. However when the value of Reynolds number is more than 4000 than the flow can be taken as turbulent. Laminar flow consists of trajectories that are smooth, regular and do not change direction. Whereas fluid flow in which the particles of the fluid keep changing direction is taken as turbulent flow [22].

Compressible and Incompressible Fluids

When the fluid density is constant inside the fluid flow then it is taken as incompressible fluid, contrarily the fluid flow is considered compressible. Incompressibility of a fluid can be expressed as

$$\frac{D\rho}{Dt} = 0 \quad (1.2)$$

here ρ is fluid density and D/Dt represents the material derivative, that can be written in the form

$$\frac{D}{Dt} = \frac{\partial}{\partial t} + \mathbf{V} \cdot \nabla$$

here \mathbf{V} is the velocity of fluid flow and ∇ is the differential operator. Here the value of ∇ in Cartesian and cylindrical coordinate systems can be given respectively as

$$\nabla = \frac{\partial}{\partial x} \hat{i} + \frac{\partial}{\partial y} \hat{j} + \frac{\partial}{\partial z} \hat{k} \quad (1.3)$$

$$\nabla = \frac{\partial}{\partial r} e_r + \frac{1}{r} \frac{\partial}{\partial \theta} e_\theta + \frac{\partial}{\partial z} e_z \quad (1.4)$$

where \hat{i} , \hat{j} and \hat{k} are unit vectors in x , y and z directions respectively and (e_r, e_θ, e_z) represent unit vector in radial, angular and axial directions respectively.

Viscosity

Viscosity of a fluid measures the fluid resistance when shear stress is applied on it. μ is the measure of the fluid viscosity and it is recognized as the viscosity coefficient. It represents proportionality constant among ratio of shear stress and the velocity gradient which can be represented in mathematical form as

$$\tau = \mu \frac{\partial v}{\partial y} \quad (1.5)$$

Viscous and Inviscid Fluids

Viscous fluids are fluids possessing a finite value of viscosity. Otherwise the fluids that have negligible amount of viscosity or viscosity is absent are considered as inviscid fluids. Generally the viscosity of a fluid is never zero but for special cases or ideal fluids, viscosity is taken to be negligible [23].

Newtonian and Non-Newtonian Fluids

The fluids that abide by Newton's law of viscosity are called Newtonian fluids. Where Newton's law of viscosity states that shear stress is linearly proportional to velocity gradient. Its mathematical form can be written as

$$\tau = \mu \frac{\partial v}{\partial y}$$

here μ is the coefficient of viscosity. Whereas fluids that disobey Newton's law of viscosity are termed as Non-Newtonian fluids. This can be mathematically written in the following form

$$\tau = k \left(\frac{\partial v}{\partial y} \right)^n$$

here k is the consistency index (it indicates the consistency of something) and n is known as the flow behavior index (it is the amount of non-Newtonian characteristic of a fluid). If we take $n = 1$ then the fluid is Newtonian, contrarily it would be non-Newtonian [22].

Bulk mean velocity

The velocity of a fluid differs at each cross section so a singular value of velocity is needed for calculations and this need is fulfilled by bulk mean velocity, when dealing with internal flows. Mathematically bulk mean velocity can be defined with the help of its relation with mass flow rate through a duct as [24].

$$\dot{m} = \rho u_m A_c, \quad (1.6)$$

where A_c is the cross sectional area of duct, ρ is the density of fluid and u_m is the bulk mean velocity which is given by

$$u_m = \frac{1}{A_c} \iint r u dr d\theta \quad (1.7)$$

1.3.2 Mathematical Models Governing Fluid Flow

Here generalized mathematical models governing fluid flow will be considered which are rooted in the law of conservation of momentum and conservation of mass.

Generalized Continuity Equation

The equation of continuity can be derived from the law of conservation of mass that is given as that rate of mass entering a system is equal to rate of mass leaving a system. The continuity equation can be mathematically expressed as [25]

$$\frac{\partial \rho}{\partial t} + \nabla \cdot (\rho \mathbf{V}) = 0 \quad (1.8)$$

Here \mathbf{V} represents the velocity of fluid and ∇ is the differential operator already discussed before in equation (1.3) and (1.4).

Generalized Momentum Equation

The momentum equation can be derived from the law regarding the conservation of momentum, which in turn is rooted in Newtons second law of motion. Generally this is

known as Navier-Stokes equation and its compact form can be penned down in three dimensional Cartesian coordinates as:

$$\rho \frac{D\mathbf{V}}{Dt} = -\nabla\mathbf{P} + \mu\nabla^2\boldsymbol{\tau} + \rho\mathbf{g} \quad (1.9)$$

here we consider \mathbf{V} as the velocity vector of fluid, ∇ is the differential operator, \mathbf{g} is the vector representing all forces on the body in three dimensions, \mathbf{P} denotes the pressure appearing over the fluid and the stress tensor appears as $\boldsymbol{\tau}$. Generally these are known as the Navier-Stokes equation and they can be expressed mathematically as [25]

$$\rho \frac{Du}{Dt} = -\frac{\partial P}{\partial x} + \frac{\partial\tau_{xx}}{\partial x} + \frac{\partial\tau_{yx}}{\partial y} + \frac{\partial\tau_{zx}}{\partial z} + \rho g_x \quad (1.10)$$

$$\rho \frac{Dv}{Dt} = -\frac{\partial P}{\partial y} + \frac{\partial\tau_{xy}}{\partial x} + \frac{\partial\tau_{yy}}{\partial y} + \frac{\partial\tau_{zy}}{\partial z} + \rho g_y \quad (1.11)$$

$$\rho \frac{Dw}{Dt} = -\frac{\partial P}{\partial z} + \frac{\partial\tau_{xz}}{\partial x} + \frac{\partial\tau_{yz}}{\partial y} + \frac{\partial\tau_{zz}}{\partial z} + \rho g_z \quad (1.12)$$

The components of $\boldsymbol{\tau}$ for Newtonian fluids, calculated by Stokes can be expressed as [25]

$$\tau_{xx} = \lambda(\nabla \cdot \mathbf{V}) + 2\mu \frac{\partial u}{\partial x} \quad (1.13)$$

$$\tau_{yy} = \lambda(\nabla \cdot \mathbf{V}) + 2\mu \frac{\partial v}{\partial y} \quad (1.14)$$

$$\tau_{zz} = \lambda(\nabla \cdot \mathbf{V}) + 2\mu \frac{\partial w}{\partial z} \quad (1.15)$$

$$\tau_{xy} = \tau_{yx} = \mu \left(\frac{\partial v}{\partial x} + \frac{\partial u}{\partial y} \right) \quad (1.16)$$

$$\tau_{zy} = \tau_{yz} = \mu \left(\frac{\partial w}{\partial y} + \frac{\partial v}{\partial z} \right) \quad (1.17)$$

$$\tau_{xz} = \tau_{zx} = \mu \left(\frac{\partial w}{\partial x} + \frac{\partial u}{\partial z} \right) \quad (1.18)$$

Where μ is the viscosity and λ is the second viscosity coefficient expressed as

$$\lambda = -\frac{2}{3}\mu \quad (1.19)$$

1.3.3 Heat Transfer

Heat transfer is a phenomenon of transferring energy due to a temperature difference in different regions. Heat is transferred from a region of higher temperature to a region of lower temperature. Whenever there exists some temperature gradient between different media or within the same medium heat transfer occurs. [24].

Heat Exchanger

Heat exchanger is a device used for the transfer or exchange of heat between two or more fluids. The fluids can be in direct connect to each other or separate by a media.

1.3.4 Modes of Heat Transfer

The modes of transferring heat can be categorized into heat transfer by *Conduction*, *Convection* and *Radiation*.

Conduction

Heat transfer with respect to conduction can be viewed as the heat transferred from one extreme temperature point to another mild temperature point within a body or between different bodies that are in contact with one another. Conduction is a heat exchange between atoms and molecules.

Heat transfer process can be analyzed with help of rate equation which calculates energy transferred per unit time. For a plane wall that is one-dimensional with temperature distribution represented by $T(x)$, conduction rate equation generally known as the Fouriers law can be written as [24]

$$q_x'' = -\kappa \frac{dT}{dx} \quad (1.20)$$

Here q_x'' denotes the heat flux (W/m^2), κ represents the thermal conductivity of wall ($W/m.K$) (thermal aspect of wall). The negative sign is present because heat is transferred from higher to lower temperature.

Convection

As the molecules of a fluid are in a constant state of motion hence the functioning of heat transfer due to convection comprises of irregular molecule movement (diffusion) that brings about energy transfer. The fluid motion, that can be bulk or macroscopic, is also responsible for energy transition. Convection occurs between boundary layer and the moving fluid when there exists a temperature difference between them as a result of the velocity and thermal boundary layer development (which is produced when a fluid and a surface, that is in contact with it, are at alternating temperatures) [24]. Thus the particles of a fluid that are directly connected with the boundary tend to attain the surface temperature hence the first heated layer of fluid transfers heat to the next layer and so on. This forms temperature gradients in fluid. Thermal boundary layer constitutes of fluid containing temperature gradients.

By definition convection consists of two processes that is heat transfer with random molecular motion and bulk motion of fluid. Heat transfer by diffusion prevails when fluid velocity is low. At the contact area between fluid and surface heat is transferred by random molecular motion (diffusion) only, because the velocity is zero. Heat transfer due to bulk motion of fluid occurs when the boundary layer progresses in the direction of flow. Ultimately the heat transferred through this layer reaches the fluid outside the boundary layer.

Convection can be *forced*, *free* or *mixed*. Forced convection occurs when the flow is caused by external factors, such as a fan, a pump, or atmospheric winds. Whereas free (natural) convection occurs due to density differences which are caused by temperature variation. For example the rising of a hot balloon and rising of smoke through chimney. Mixed convection occurs when free and forced convection work together to transmit heat. For example a fan blowing air on a heated plate in upward direction. Latent heat exchange can cause convection which is commonly associated to a phase alternation in a fluid that occurs among the liquid and vapor states. Boiling and condensation processes can be

involved in this.

Despite the nature of the convection heat transfer process, the appropriate rate equation is of the form:

$$\dot{q}'' = h(T_s - T_\infty) \quad (1.21)$$

which is known as Newton's law of cooling [24], where \dot{q}'' is the convective heat flux (W/m^2), where h ($W/m^2.K$) is the convection heat transfer coefficient, T_s and T_∞ are the surface and fluid temperatures respectively.

Radiation

Radiation is a process in which energy is emitted from matter at non-zero temperatures in form of electromagnetic waves, particles or rays by matter [24]. Solids and liquids, both states can exhibit the phenomenon of radiation. Electromagnetic waves transmit the energy that is created by radiation process. Radiation process can occur without the aid of any medium. So radiation is more efficient in vacuum.

1.3.5 Bulk mean temperature

Just like velocity of a fluid, at each cross section the temperature of a fluid also changes hence bulk mean temperature is required. It can be represented by T_b and it is defined as

$$T_b = \frac{1}{u_m A_c} \iint u T r dr d\theta \quad (1.22)$$

Where u_m represents the bulk mean velocity of a fluid, T is associated with fluid temperature and A_c gives the cross sectional area of computational domain.

1.3.6 Generalized Energy Equation

The first law of thermodynamics can be generalized to form energy equation. It could be understood from the first law of thermodynamics that the rate of change of energy within an element of fluid is same as the sum of net flux of heat into element and rate

of work done on the element due to body and surface forces. The energy equation in non-conservation form can be written as [25]

$$\begin{aligned} \rho \frac{D}{Dt} \left(e + \frac{V^2}{2} \right) = \rho \dot{q} + \frac{\partial}{\partial x} \left(k \frac{\partial T}{\partial x} \right) + \frac{\partial}{\partial y} \left(k \frac{\partial T}{\partial y} \right) + \frac{\partial}{\partial z} \left(k \frac{\partial T}{\partial z} \right) - \frac{\partial u p}{\partial x} - \frac{\partial v p}{\partial y} - \frac{\partial w p}{\partial z} \\ + \frac{\partial u \tau_{xx}}{\partial x} + \frac{\partial u \tau_{yx}}{\partial y} + \frac{\partial u \tau_{zx}}{\partial z} + \frac{\partial v \tau_{xy}}{\partial x} + \frac{\partial v \tau_{yy}}{\partial y} + \frac{\partial v \tau_{zy}}{\partial z} + \frac{\partial w \tau_{xx}}{\partial x} + \frac{\partial w \tau_{yx}}{\partial y} + \frac{\partial w \tau_{zz}}{\partial z} + \rho \mathbf{g} \cdot \mathbf{V} \end{aligned} \quad (1.23)$$

here T represents the fluid temperature, μ gives the density of the fluid and τ represents the stress tensors whose components are given by equations (1.13)-(1.18) as mentioned earlier.

1.3.7 Fluid Flow and Heat Transfer Parameters

In this section, we will discuss some parameters that are important for the understanding of this research.

Hydraulic Diameter

It is the characteristic length of any duct regardless of its shape. It can be described as the ratio between cross sectional area and wetted parameter [24].

$$D_h = 4 \frac{A_c}{p_w} \quad (1.24)$$

where A_c is cross sectional area and p_w is the wetted parameter of the duct.

Dimensionless Quantities

They are pure numbers that are deficient of physical unit. Dimensionless quantities can be represented in product or fraction form of quantities that have physical units but all their units are canceled off each other to form a dimensionless quantity. Dimensionless quantities are very helpful in comparing different systems and determining the behavior of a system. They can also simplify the solution finding process of a system.

Reynolds Number

It is a non-dimensional quantity. Reynolds number (Re) is taken as the ratio from inertia to viscous forces. If Reynolds number is small it shows that the forces of inertia are less than viscous forces thus resulting in a laminar flow whereas if it is large then the flow is turbulent as the viscous forces are less than inertia forces. It can be written as [24]

$$Re = \frac{u_m D_h}{\nu} \quad (1.25)$$

here u_m represents the fluid's bulk mean velocity, D_h serves as the hydraulic diameter whereas $\nu = \frac{\mu}{\rho}$.

Fanning Friction Factor

It describes the ratio between shearing stress and kinetic energy density of local flow. It is applied in the calculations of fluid flow. It can be written as [24]

$$f = \frac{\tau_s}{\frac{\rho u_m^2}{2}} \quad (1.26)$$

Where τ_s is the stress exerted on wall and its expression is given as

$$\tau_s = -\mu \left(\frac{du}{dr} \right)_{r=r_o} \quad (1.27)$$

The term fRe , that describes the multiplication of fanning friction factor to Reynolds number, is employed for the calculation of friction present in fluid flow. It can be written as

$$fRe = -\frac{dP}{2\mu dz} \frac{D_h^2}{u_m} \quad (1.28)$$

Nusselt Number

It is a dimensionless quantity and it is the ratio of heat transfer by convection and heat transfer by conduction. A large Nusselt number means convection is more than conduction and a small Nusselt number shows more amount of conduction than convection. Larger the

Nusselt number, higher would be the transfer of heat. Nusselt number can be represented by the following equation [24]

$$Nu = \frac{hL}{\kappa} \quad (1.29)$$

Where h is convective heat transfer coefficient, L is diameter of ducts and κ is the thermal conductivity. It can be observed that Nusselt number is equal to the value of dimensionless temperature gradient at the surface and it is employed to measure heat transfer due to convection at the surface.

Prandtl Number

Prandtl number describes a dimensionless quantity which is the ratio of momentum diffusivity (it is the ratio of viscosity coefficient to density of fluid) to thermal diffusivity (it is the thermal conductivity of a medium divided by density and specific heat capacity). It approximates the dominance of conduction or convection in a fluid flow. It can be expressed as [24]

$$Pr = \frac{\nu}{\beta} = \frac{\mu c_p}{\kappa} \quad (1.30)$$

here absolute or dynamic viscosity is represented by μ , c_p depicts the specific heat capacity whereas κ expresses thermal conductivity.

J Factor

Colburn's j factor is a non-dimensional quantity which is an analogy that relates heat transfer coefficients, mass transfer coefficients and friction factor. It can be expressed in mathematical form as [34]

$$jfactor = \frac{NuPr^{-\frac{1}{3}}}{fRe} \quad (1.31)$$

here Pr is the Prandth number which is a dimensionless quantity that is the ratio between momentum diffusivity to thermal diffusivity. Its mathematically expression can be seen through equation (1.30). J factor is very significant in our research as it provides a direct correlation between Nu and fRe , later this would help us in the optimization of results.

1.3.8 Boundary Conditions

Boundary conditions are important in the search of a mathematical solution of any problem. A few boundary conditions are given as

Velocity Boundary Conditions

There is a variety of boundary conditions available for finite volume method. A few of the most commonly used of them are: inlet, outlet and wall boundary conditions. Inlet boundary condition suggests that all the flow variables must be described at the inlet boundaries, especially velocity. Outlet boundary condition is similar to inlet boundary condition except that flow variables must be specified at the outlet of a duct. When no disturbance occurs in the flow than flow turns to be full developed flow and an outlet can be introduced there. The gradient of velocity is taken to be equal to zero at the outlet parallel to the flow direction. Wall boundary condition commonly known as no-slip condition describes that during the course of a fluid flow when an inviscid fluid passes over any firm fixed obstruction then it is essential for the normal velocity of fluid, which is at the surface of the obstacle, to be zero. Customarily, the tangential velocity of a fluid has some finite value. So when we observe the interaction of a viscous fluid with a firm fixed obstruction, it can be noted that the normal and tangential components of its velocity turn out to be zero at the surface of the obstruction. This case where both the vertical and tangential velocity component of fluid is zero is called no slip condition [26].

Thermal Boundary Conditions

A number of boundary conditions can be applied on the inner walls of a duct. We will discuss four main thermal boundary conditions here, that is H_1 , H_2 , T . H_1 boundary condition [28] implicates a constant axial heat flux per unit length of the duct along with a steady peripheral temperature of the duct's heated surface. Hence by this condition it can be understood that there is infinite heat conduction by the surface of duct in the

radial and transverse directions but heat conduction is negligible in axial direction. It can be suggested for highly conductive ducts with small peripheral temperature gradients. Whereas H_2 boundary implies that wall heat transfer rate should be constant axially and peripheral, at every cross section. T [27] boundary condition suggests that the wall temperature is kept constant through the peripheral and axial length of the duct wall. This boundary condition is applied usually on evaporators, condensers and high velocity flow liquid to gas heat exchangers.

1.3.9 Boundary Layers

The boundary layer notion is important for the understanding of convective heat transfer from a heated surface to the fluid passing over it. In this section the concept of velocity and thermal boundary layers is explained.

Velocity Boundary Layer

Due to no slip condition when fluid particles pass over a surface, the particles in contact with the surface acquire zero velocity. These particles then obstruct the motion of the particles of the next fluid layer and this action passes on to the next layer until at a finite distance from the surface, the retardation effect becomes negligible. As the distance of the fluid particles, from the bounding surface increases the axial component of velocity increases from zero to the free stream value of velocity. Hence fluid flow can be categorized into two different regions, the boundary layer through which the velocity gradient and shear stresses are large and another region outside the boundary layer where velocity gradient and shear stress are negligible. As the distance from surface increases the thickness of the boundary layer becomes large. As this boundary layer is relevant to fluid velocity so it is specified as velocity boundary layer [24].

Thermal Boundary Layer

The concept of thermal boundary layer is relevant to the concept of velocity boundary layer. The fluid particles that are in direct contact with the heated surface assume the temperature of that surface. Then these particles exchange energy with the adjoining fluid layer and this energy is in turn passed on to the next layer hence a temperature gradient is formed. The fluid region containing these temperature gradients is known as the thermal boundary layer [24].

Chapter 2

Solution Strategies

2.1 Introduction

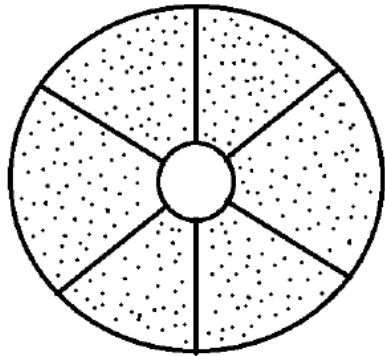
In this chapter, the solution strategies of fluid flow and heat transfer will be discussed. Where the fluid is considered to be Newtonian, that is flowing through an annular sector duct packed with Darcy-Brinkman's porous media. Constant heat flux boundary conditions were applied to model the problem, as it was discussed earlier by M. Iqbal and H. Afaq [21]. They observed the presence of an optimal geometry for which a separate study should be carried out. The presence of this optimal geometry suggests the occurrence of a duct configuration for which heat transfer rate is maximum along with a minimum friction effect. To find such a geometry optimization techniques namely trust region method and genetic algorithm would be analyzed and later we will choose a technique for the optimization of our problem. Also results have been validated with literature.

2.2 Problem Formulation

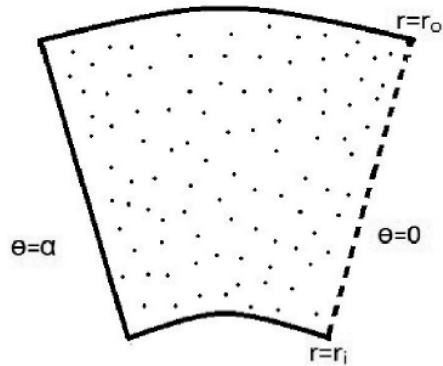
Lets study a steady state, laminar flow that is thermally and hydro-dynamically fully developed. The fluid is taken to be incompressible, viscous and Newtonian flowing through an annular sector duct packed with Darcy-Brinkmans porous media. Vertical fins are

inserted in the ducts annulus between the external and internal pipe (as displayed by figure 2.1a). The radius of internal and external pipe is considered to be r_i and r_o respectively and the sector angle that is the angle between two consecutive fins is taken as 2α . Geometrical symmetry can be observed in the figure 2.1a, on account of that the computational domain is considered as half of the region that is contained between successive fins (seen through figure 2.1b). Hence computational sector angle is taken as α and sector length is represented by $r_o - r_i$. Forced convection is carried out by moving heated fluid through inner pipe whereas cold fluid through outer pipe synchronously. The outer pipes external surface is insulated to prevent heat loss across this surface. Hence the only heat transferring surfaces are the inner pipe and longitudinal fins.

The modeling of the problem undergoes constant heat flux boundary conditions, commonly known as H_1 boundary conditions [28], that are applied on the inner side of the heat transferring surfaces. The only driving force is taken as constant pressure gradient in the axial direction.



(a) Cross-sectional view of concentric pipes



(b) Computational domain

Figure 2.1: Geometry of duct

The conservation relations of mass and momentum along with the continuity equation can be written in the cylindrical polar coordinates as:

Continuity Equation

$$\frac{\partial \rho}{\partial t} + \frac{\partial(\rho r u)}{r \partial r} + \frac{\partial \rho v}{r \partial \theta} + \frac{\partial \rho w}{\partial z} = 0 \quad (2.1)$$

Momentum Equations

Momentum equations are defined as

$$\begin{aligned} \rho \left(\frac{\partial u}{\partial t} + u \frac{\partial u}{\partial r} + \frac{v}{r} \frac{\partial u}{\partial \theta} + w \frac{\partial u}{\partial z} - \frac{v^2}{r} \right) = & -\frac{\partial P}{\partial r} + \mu \left[\frac{\partial}{r \partial r} \left(r \frac{\partial u}{\partial r} \right) + \frac{1}{r^2} \frac{\partial^2 u}{\partial \theta^2} \right] \\ & + \mu \left[\frac{\partial^2 u}{\partial z^2} - \frac{u}{r^2} - \frac{2}{r^2} \frac{\partial v}{\partial \theta} \right] + \rho g_r \end{aligned} \quad (2.2)$$

$$\begin{aligned} \rho \left(\frac{\partial v}{\partial t} + u \frac{\partial v}{\partial r} + \frac{v}{r} \frac{\partial v}{\partial \theta} + w \frac{\partial v}{\partial z} - \frac{uv}{r} \right) = & -\frac{1}{r} \frac{\partial P}{\partial \theta} + \mu \left(\frac{\partial}{r \partial r} \left(r \frac{\partial v}{\partial r} \right) \right) \\ & + \mu \left(\frac{1}{r^2} \frac{\partial^2 v}{\partial \theta^2} + \frac{\partial^2 v}{\partial z^2} - \frac{v}{r^2} + \frac{2}{r^2} \frac{\partial u}{\partial \theta} \right) + \rho g_\theta \end{aligned} \quad (2.3)$$

$$\rho \left(\frac{\partial w}{\partial t} + u \frac{\partial w}{\partial r} + \frac{v}{r} \frac{\partial w}{\partial \theta} + w \frac{\partial w}{\partial z} \right) = -\frac{\partial P}{\partial z} + \mu \left(\frac{\partial}{r \partial r} \left(r \frac{\partial w}{\partial r} \right) \right) + \mu \left(\frac{1}{r^2} \frac{\partial^2 w}{\partial \theta^2} + \frac{\partial^2 w}{\partial z^2} \right) + \rho g_z \quad (2.4)$$

The Darcy-Brinkmans conservation relations for momentum can be viewed in the cylindrical polar coordinates as [21]. Momentum equations in cylindrical polar coordinates for Darcy-Brinkman's porous media can be written as:

$$\begin{aligned} \rho \left(\frac{\partial u}{\partial t} + u \frac{\partial u}{\partial r} + \frac{v}{r} \frac{\partial u}{\partial \theta} + w \frac{\partial u}{\partial z} - \frac{v^2}{r} \right) = & -\frac{\partial P}{\partial r} + \mu \left[\frac{\partial}{r \partial r} \left(r \frac{\partial u}{\partial r} \right) \right] \\ & + \mu \left(\frac{1}{r^2} \frac{\partial^2 u}{\partial \theta^2} + \frac{\partial^2 u}{\partial z^2} - \frac{u}{r^2} - \frac{2}{r^2} \frac{\partial v}{\partial \theta} - \frac{u}{K} \right) + \rho g_r \end{aligned} \quad (2.5)$$

$$\begin{aligned} \rho \left(\frac{\partial v}{\partial t} + u \frac{\partial v}{\partial r} + \frac{v}{r} \frac{\partial v}{\partial \theta} + w \frac{\partial v}{\partial z} - \frac{uv}{r} \right) = & -\frac{1}{r} \frac{\partial P}{\partial \theta} + \mu \left(\frac{\partial}{r \partial r} \left(r \frac{\partial v}{\partial r} \right) \right) \\ & + \mu \left(\frac{1}{r^2} \frac{\partial^2 v}{\partial \theta^2} + \frac{\partial^2 v}{\partial z^2} - \frac{v}{r^2} + \frac{2}{r^2} \frac{\partial u}{\partial \theta} - \frac{v}{K} \right) + \rho g_\theta \end{aligned} \quad (2.6)$$

$$\rho \left(\frac{\partial w}{\partial t} + u \frac{\partial w}{\partial r} + \frac{v}{r} \frac{\partial w}{\partial \theta} + w \frac{\partial w}{\partial z} \right) = -\frac{\partial P}{\partial z} + \mu \left(\frac{\partial}{r \partial r} \left(r \frac{\partial w}{\partial r} \right) \right) + \mu \left(\frac{1}{r^2} \frac{\partial^2 w}{\partial \theta^2} + \frac{\partial^2 w}{\partial z^2} - \frac{w}{K} \right) + \rho g_z \quad (2.7)$$

In the above equations, K is considered as the permeability of the medium, ρ is density of the medium (fluid), (u, v, w) are the velocity components of the fluid, \mathbf{P} is the pressure exerted by the fluid, μ is the dynamic viscosity and (g_r, g_θ, g_z) are components the gravitational vector on the fluid or it can be summed up as the body forces on the fluid. After the application of the geometric conditions and assumptions for this study, the continuity equation is satisfied and momentum equations reduce to

$$\frac{\partial P}{\partial r} = 0 \quad (2.8)$$

$$\frac{\partial P}{\partial \theta} = 0 \quad (2.9)$$

$$\mu \left(\frac{\partial}{r \partial r} \left(r \frac{\partial w}{\partial r} \right) + \frac{1}{r^2} \frac{\partial^2 w}{\partial \theta^2} - \frac{w}{K} \right) - \frac{\partial P}{\partial z} = 0 \quad (2.10)$$

The equations (2.8) and (2.9) show the absence of pressure gradient in radial (r) and angular (θ) directions. Hence the expression given in (2.10) can be reduced as

$$\frac{\partial^2 w}{\partial r^2} + \frac{1}{r} \frac{\partial w}{\partial r} + \frac{1}{r^2} \frac{\partial^2 w}{\partial \theta^2} - \frac{w}{K} = \frac{1}{\mu} \frac{\partial P}{\partial z} \quad (2.11)$$

Where the prescribed boundary conditions on reduced momentum equation are

$$\text{for } r = r_i, \quad w = 0 \quad 0 \leq \theta \leq \alpha \quad (2.12)$$

$$\text{for } r = r_o, \quad w = 0 \quad 0 \leq \theta \leq \alpha \quad (2.13)$$

$$\text{for } \theta = 0, \quad \frac{\partial w}{\partial \theta} = 0 \quad r_i \leq r \leq r_o \quad (2.14)$$

$$\text{for } \theta = \alpha, \quad w = 0 \quad r_i \leq r \leq r_o \quad (2.15)$$

To make above reduced momentum equation and its boundary equations dimensionless we introduce the following parameters

$$R = \frac{r}{r_o} \quad \tilde{R} = \frac{r_i}{r_o} \quad (2.16)$$

$$\hat{w} = -\frac{w}{\frac{1}{\mu} r_o^2 \frac{\partial P}{\partial z}} \quad \hat{K} = \frac{K}{r_o^2} \quad (2.17)$$

Here \hat{K} is Darcy number. So now with the help of above parameters (2.16) and (2.17), the dimensionless momentum equation could be expressed in the following form

$$\frac{\partial^2 \hat{w}}{\partial R^2} + \frac{1}{R} \frac{\partial \hat{w}}{\partial R} + \frac{1}{R^2} \frac{\partial^2 \hat{w}}{\partial \theta^2} - \frac{\hat{w}}{\hat{K}} = -1 \quad (2.18)$$

The boundary conditions are now transformed into

$$\text{for } R = \tilde{R}, \quad \hat{w} = 0 \quad 0 \leq \theta \leq \alpha \quad (2.19)$$

$$\text{at } R = 1, \quad \hat{w} = 0 \quad 0 \leq \theta \leq \alpha \quad (2.20)$$

$$\text{at } \theta = 0, \quad \frac{\partial \hat{w}}{\partial \theta} = 0 \quad r_i \leq r \leq r_o \quad (2.21)$$

$$\text{at } \theta = \alpha, \quad \hat{w} = 0 \quad r_i \leq r \leq r_o \quad (2.22)$$

Energy Equation

The energy equation can be used to observe the heat transfer through a fluid flow. For cylindrical polar coordinates it can be expressed as

$$\rho c_p \left(\frac{\partial T}{\partial t} + u \frac{\partial T}{\partial r} + \frac{v}{r} \frac{\partial T}{\partial \theta} + w \frac{\partial T}{\partial z} \right) = \kappa \left(\frac{\partial^2 T}{\partial r^2} + \frac{1}{r} \frac{\partial T}{\partial r} + \frac{1}{r^2} \frac{\partial^2 T}{\partial \theta^2} + \frac{\partial^2 T}{\partial z^2} \right) \quad (2.23)$$

where ρ is taken as the density of fluid, κ is the thermal conductivity of fluid and c_p as the specific heat capacity. Due to assumptions taken for this study the energy equation can be reduced to

$$\frac{\partial^2 T}{\partial r^2} + \frac{1}{r} \frac{\partial T}{\partial r} + \frac{1}{r^2} \frac{\partial^2 T}{\partial \theta^2} = \frac{\rho c_p}{\kappa} \left(w \frac{\partial T}{\partial z} \right) \quad (2.24)$$

The boundary conditions for the governing equation can be written in the following from

$$T = T_w(z) \quad \text{at} \quad r = r_i, \quad 0 \leq \theta \leq \alpha \quad (2.25)$$

$$\frac{\partial T}{\partial r} = 0 \quad \text{at} \quad r = r_o, \quad 0 \leq \theta \leq \alpha \quad (2.26)$$

$$\frac{\partial T}{\partial \theta} = 0 \quad \text{at} \quad \theta = 0, \quad r_i \leq r \leq r_o \quad (2.27)$$

$$T = T_w(z), \quad \text{at} \quad \theta = \alpha, \quad r_i \leq r \leq r_o \quad (2.28)$$

where T_w is taken as the wall temperature that varies axially with the coordinate z , for a constant rate of heat throughout the pipe. For a smooth heat transfer the temperature distribution and wall temperature should be different and alter axially. For a temperature field independent of axial coordinate we form a non-dimensional parameter τ , where the flow is taken to be thermally fully developed.

$$\tau = \frac{T - T_W}{\frac{q'}{\kappa}} \quad (2.29)$$

Here q' is taken as heat transfer rate per unit length in axial direction of duct. After incorporating τ into energy equation (2.24) it reduces to

$$\frac{\partial^2 T}{\partial r^2} + \frac{1}{r} \frac{\partial T}{\partial r} + \frac{1}{r^2} \frac{\partial^2 T}{\partial \theta^2} = \frac{w}{A_c w_m} \frac{q'}{K} \quad (2.30)$$

To make reduced energy equation and its boundary equations dimensionless we introduce the same parameters as given in (2.16) and (2.17). Hence (2.30) in non-dimensional form is expressed as.

$$\frac{\partial^2 \tau}{\partial R^2} + \frac{1}{R} \frac{\partial \tau}{\partial R} + \frac{1}{R^2} \frac{\partial^2 \tau}{\partial \theta^2} = \frac{\hat{w}}{A_c \hat{w}_m} \quad (2.31)$$

Where \hat{w}_m represents the non-dimensional mean velocity. The dimensionless parameters transform the boundary conditions (2.25)-(2.28) of energy equation into:

$$\text{at} \quad R = \tilde{R}, \quad \tau = 0 \quad , \quad 0 \leq \theta \leq \alpha \quad (2.32)$$

$$\text{at } R = 1, \quad \frac{\partial \tau}{\partial R} = 0 \quad , \quad 0 \leq \theta \leq \alpha \quad (2.33)$$

$$\text{at } \theta = 0, \quad \frac{\partial \tau}{\partial \theta} = 0 \quad , \quad \tilde{R} \leq R \leq 1 \quad (2.34)$$

$$\text{at } \theta = \alpha, \quad \tau = 0, \quad , \quad \tilde{R} \leq R \leq 1 \quad (2.35)$$

2.3 Discretization

Finite difference method (FDM) is employed to discretize the governing equations (2.18) and (2.31) by applying five point stencil with second order approximations, which are given as

$$\frac{\partial^2 w}{\partial R^2} = \frac{w(i+1, j) - 2w(i, j) + w(i-1, j)}{h^2} + O(h^2) \quad (2.36)$$

$$\frac{\partial^2 w}{\partial \theta^2} = \frac{w(i, j+1) - 2w(i, j) + w(i, j-1)}{k^2} + O(k^2) \quad (2.37)$$

$$\frac{\partial w}{\partial R} = \frac{w(i+1, j) - w(i-1, j)}{2h} + O(h^2) \quad (2.38)$$

Whereas the same discretization are valid for energy equation with slight adjustments.

$$\frac{\partial^2 \tau}{\partial R^2} = \frac{\tau(i+1, j) - 2\tau(i, j) + \tau(i-1, j)}{h^2} + O(h^2) \quad (2.39)$$

$$\frac{\partial^2 \tau}{\partial \theta^2} = \frac{\tau(i, j+1) - 2\tau(i, j) + \tau(i, j-1)}{k^2} + O(k^2) \quad (2.40)$$

$$\frac{\partial \tau}{\partial R} = \frac{\tau(i+1, j) - \tau(i-1, j)}{2h} + O(h^2) \quad (2.41)$$

Here h and k represent the size of a step in R and θ direction respectively. The above approximations can be placed in governing equations and later they can be simplified using a numerical technique called SOR method.

2.4 Numerical Technique

Successive Over Relaxation (SOR) method is employed to solve the discretized equation.

The general form of SOR method can be written as

$$X_i^{(k+1)} = (1 - \omega)X_i^k + \frac{\omega}{a_{ii}}(b_i - \sum_{j=1}^{i-1} a_{ij}x_j^{(k+1)} - \sum_{j=i}^n a_{ij}x_j^k) \quad (2.42)$$

Where ω is the relaxation factor. a_{ii} , a_{ij} , b_i and k are constants. All computations have been done in MATLAB.

2.5 Validation of Results

In this section we have conducted a comparison of the calculated values of fRe and Nu for present study, with those already present in literature [21]. With the help of table 2.1 we demonstrate the calculated and literature value comparison for Nu where $\tilde{R} = 0.25$, $\tilde{R} = 0.5$ and α is taken as 0.524.

The table 2.2 is used to evaluates the comparison for fRe where we consider values for $\tilde{R} = 0.25$, $\tilde{R} = 0.5$ and α is taken as 1.047.

Table 2.1: Validation of results for $\hat{K} = 100$ and $\hat{K} = 0.001$ at $\alpha = 0.524$

\hat{K}	\tilde{R}	Nu		% change in Nu
		Calculated	literature	
100	0.25	3.3505	3.3494	0.03
	0.5	3.0750	3.0740	0.03
0.001	0.25	4.2392	4.2315	0.18
	0.5	3.8129	3.8049	0.2

The tables 2.1 and 2.2 both help to demonstrate that the % change for fRe and Nu calculated in present study is lower than 1% hence it can be concluded that the calculations

Table 2.2: Validation of results for $\hat{K} = 100$ and $\hat{K} = 0.001$ at $\alpha = 1.047$

\hat{K}	\tilde{R}	fRe		% change in fRe
		Calculated	literature	
100	0.25	15.2551	15.2591	0.03
	0.5	17.2364	17.2436	0.04
0.001	0.25	518.5591	519.7828	0.24
	0.5	341.6646	342.5348	0.25

made are correct and have a high compatibility with literature.

2.6 Optimization Methods

In this section we will study two methods for the optimization i.e Genetic Algorithm (GA) and Trust Region Method (TRM) and select one out of these to be used for our research problem. Both techniques have totally different frame work to leave no doubt in our conclusion; Genetic algorithm is of probabilistic nature whereas trust region method is deterministic in character. The implementation of these techniques helps to determine their efficiency and other traits for optimizing a problem. We execute these procedures for optimization using mathematical codes in MATLAB. To understand the optimization techniques better their general frame-work is discussed below.

Trust Region Method (TRM)

Trust region method [30,31] is an iterative numerical algorithm that is widely used for optimization of non-linear convex problems. It can work with both constrained and unconstrained problems. They are quite popular due to their robust nature, fast convergence rate and application to ill-conditioned problems. By default trust region method tries to locate a region of trust around an initial point in which it trusts to find the optimum

value. This trust region is usually a neighborhood centered at the current base point. It approximates the optimum value of the problem, within the trust region by using a quadratic model problem that reflects on the behavior of the main objective function. The approximations are made by employing second order Taylor series. The two-dimensional subproblem has a variety of exact and approximate methods to reach it's solution. A general characterization of trust region method for constrained mathematical optimization is discussed below.

Lets examine a problem that has to be minimized, with bounds on its parameter

$$f(x), \quad \text{where } x \in R^n \quad (2.43)$$

$$lb \leq x \leq ub \quad (2.44)$$

Here R^n is the domain in which optimum value of $f(x)$ is investigated; lb and ub are lower and upper bounds of $f(x)$ respectively. For simplification we first discuss trust region method for unconstrained problem so the bound constraints given in equation 2.44 is ignored for now. While considering a unconstrained optimization, its constrained sub-problem can be written in the form

$$\min_q \{m_k(q) = f_k + q^T g_k + \frac{1}{2} q^T H_k q, \text{ s.t. } \|D_k q\|_2 \leq \Delta_k\} \quad (2.45)$$

Here D_k represents the diagonal scaling matrix whereas Δ_k describes the scalar radius associated with trust region on its k-th iteration. This model problem is then restricted to the trust region and solved for it. A overlook of the general steps for trust region algorithm for unconstrained problems can be described as:

1. First let $\Delta_1 > 0$, $k=1$ then chose the initial point x_1 . The algorithm heuristically choses four constants $\zeta_1, \zeta_2; \delta_1, \delta_2$ that fulfill the condition that $0 < \zeta_1 \leq \zeta_2 < 1$ and $0 < \delta_1 \leq \delta_2 < 1$. The usual choice for $\zeta_1 = 0.1, \zeta_2 = 0.9$ and $\delta_1 = \delta_2 = 0.5$.
2. Construct a quadratic model subproblem for your original problem with the help of equation 2.45. Simplify the model problem to find the trial step value of q .

3. Now the algorithm determines $f(x_k + q)$ and sets a reduction model ϱ_k of f where

$$\varrho_k = \frac{f(x_k) - f(x_k + q)}{m_k(x_k) - m_k(x_k + q)} \quad (2.46)$$

Now if the value of

$$f(x_k + q) < f(x_k) \quad (2.47)$$

along with $\zeta_2 \leq \varrho_k$ then the algorithm concludes that a good quadratic model was constructed and the step that is considered is valid, that is $x_{k+1} = x_k + q$, hence the region of trust could now be expanded; otherwise if equation (2.47) holds and $\zeta_1 \leq \varrho_k < \zeta_2$ then q is taken to be a valid step and the base/center point becomes $x_{k+1} = x_k + q$ but the trust region shrinks and if equation (2.47) holds but $\zeta_1 > \varrho_k$ then the step is dismissed and worked out again and the base point remains constant i.e $x_{k+1} = x_k$.

4. The trust region radius is upgraded with each iteration, with the increase or decrease in the size of trust region. This process is repeated until the algorithm achieves convergence. Where

$$\text{Set } \Delta_{k+1} = \begin{cases} [\Delta_k, \infty) & \text{if } \varrho_k \geq \zeta_2 \\ [\delta_2 \Delta_k, \Delta_k] & \text{if } \varrho_k \in [\zeta_1, \zeta_2) \\ [\delta_1 \Delta_k, \delta_2 \Delta_k] & \text{if } \varrho_k < \zeta_1 \end{cases} \quad (2.48)$$

After the unconstrained problem we go back to equation 2.43 and 2.44 to analyze a constrained problem. The lower and upper bound vectors can have the values of their components ranging to negative and positive infinity respectively. This method is employed to form a string of feasible points. Through each iteration the robustness and feasibility can be retained by scaling of the modified Newton step which is based on Kuhn-Tucker's condition [32] and expansion in step size is caused by reflections.

The scaling of the modified Newtons step can be achieved through Kuhn-Tucker's necessary condition for 2.43 and 2.44.

$$(D(x))^{-2}g_k = 0 \quad (2.49)$$

Here the value of $D(x)$ is

$$D(x_k) = \text{diag}(|v_k|^{\frac{-1}{2}}) \quad (2.50)$$

For $1 \leq i \leq n$, the vector $v_k = v(x_k)$ can be described as

1. If $g_i < 0$ and $ub_i < \infty$ then $v_i = x_i - ub_i$
2. If $g_i \geq 0$ and $lb_i > -\infty$ then $v_i = x_i - lb_i$
3. If $g_i < 0$ and $ub_i = \infty$ then $v_i = -1$
4. If $g_i \geq 0$ and $lb_i = -\infty$ then $v_i = 1$

As a non-linear system of equations 2.49 is not necessarily differentiability all over its domain hence this non-differentiability, which occurs when $v_i = 0$ can be prevented by confining x_k i.e. $lb < x_k < ub$. The scaled modified Newton step q_k defined for a non-linear system 2.49 is taken as a solution to the following linear system, at its k-th iteration

$$\hat{M}_k D_k q_k^N(x_k) = -\hat{g}_k \quad (2.51)$$

Here we can describe see that $\hat{g}_k = D_k^{-1} g_k = \text{diag}(|v_k|^{\frac{1}{2}}) g_k$ and $\hat{M}_k = D_k^{-1} H_k D_k^{-1} + \text{diag}(g_k) J_k^v$. It is observed that $J^v(x) \in \mathbb{R}^{n \times n}$ is the Jacobian of $|v(x)|$. When the value of every component of lb and ub vectors is finite then the Jacobian is found to be $J^v = \text{diag}(\text{sign}(g_k))$. For $v_i = 0$ we can denote $j_{ii}^v = 1$. For a point where the value of $g_i = 0$, v_i is not necessarily differentiable then we can take $j_{ii}^v = 0$ at that point. But we can ignore this kind of non-differentiable behavior because of the insignificance of the value of v_i . Also v_i is discontinuous at this particular point but $|v_i|.g_i$ shows a continuous behavior. As mentioned before the step size can be expanded by employing refractions, that can be described with regard to a distinct step by: When there exists a step p which intersects through a bounded constraint hence we can write reflection step as

$$\begin{cases} p^R = p & \text{apart from } i\text{-th component} \\ p_i^R = -p_i & \text{for } i\text{-th component} \end{cases} \quad (2.52)$$

Here when p crosses the first bounded constraint it is considered as the i -th bound, it can be upper or lower bound. There are a number of stopping criteria used by trust region algorithm. For this study the stopping criteria are taken as

1. The tolerance of the function is more than the value of first-order optimality and tolerance is more than maximum constraint violation.
2. The difference in successive values of x or objective function is smaller than the tolerance.
3. The constraints are satisfied within the default constraint tolerance value.

The function trust region method have a number of limitations that make it difficult for the implementation of this numerical optimization technique. The limitations are listed below as

1. TRM may deliver local minimal or maximal point.
2. For trust region reflective algorithm, a gradient in the function is needed.
3. Also the trust region reflective algorithm does not let upper and lower bounds to be equal.

2.6.1 Genetic Algorithm

Genetic algorithm (GA) [16,29] is a global search procedure used to solve both constrained and unconstrained optimization problems. It is inspired from Darwin's theory of evolution. It belongs to the class of Evolutionary Algorithms (EA) and applies almost the same technique as EA to optimize the solution by natural selection and survival of the fittest. For each iteration the GA selects random parents/points from population/domain to generate offspring, which if satisfy the stopping criteria provide solution to the optimization problem but if not then the next iteration starts. Hence gradually the points proceed towards an optimum solution. The general outline of the algorithm can be constructed as

1. Generation

Genetic algorithm starts off by creating a random initial population from the variables.

2. Fitness Evaluation

GA creates new populations, from the old population, at each iteration by determining the fitness value ($f(x)$) of every point in current population that can be expressed as $f(x) \forall x \in population(oldgeneration)$.

3. Reproduction

The next fresh generation is created through the following steps:

(a) Selection

The fitness values are converted into an adaptable range of values and parent points are selected from the data. These parents are chosen on the basis of selection criteria such as roulette wheel selection, tournament selection etc and are called elites. These elites are then passed to the next generation. Offspring points are then created either by mutation or crossover.

(b) Crossing-over

The elite pair of parent generation is then spliced to form new off-spring generation by combining the good attributes of a parent pair. Without crossover of parent pair the new points/children generated will be a replica of their parents. A few customary operators applied for crossing-over are point, arithmetic, linear, and heuristic crossover.

(c) Mutation

Based on probability off-springs are mutated by making random changes to a parent.

(d) Acceptation

The offspring replaces their parents thus forming a new generation.

4. Stopping Criteria

The algorithm moves to evaluating the fitness value of each new generation and repeats all steps until stopping criteria is met.

Genetic algorithm is favored for optimization over other procedures due to its accuracy and reliable nature. Because GA works on many points in the domain relative to the objective function so it escapes local maxima and minima and strives for global minima. The objective function does not necessarily need to be in refined form or in specific formula, GA can work directly on domain points and fitness values can be gained with help of experimentation. It can work quite efficiently to solve large scale problem.

On the other hand every technique has its short comings some of them can be mentioned as GA is expensive. Sometimes it can take days to reach the convergence/stopping criteria. Ever now and then premature convergence occurs that disrupts the search of global optimum. It has a high probability to reach global optimum but it is an undirected search due to generation of a random initial population so it cannot always be directed towards optimal solution area.

2.6.2 GA and TRM : A Comparison

A single optimization technique can not be adopted for all problems hence we have to chose the more suitable method according to our problem, its constraints and the limitations of that technique. Here we will consider a simple problem, apply both genetic algorithm and trust region method to compare their properties and results by employing MATLAB platform. This will facilitate us in determining which method is more suitable for our problem.

Sample Problem

Let us consider a objective function or fitness function as

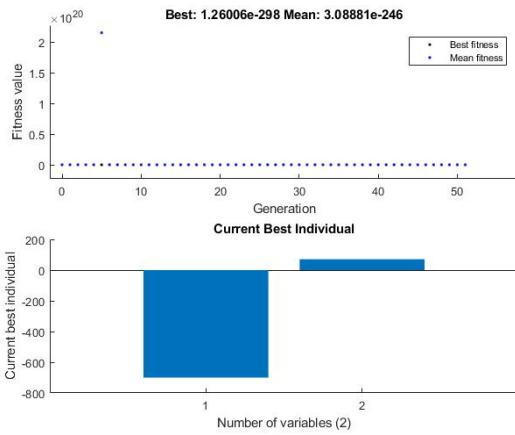
$$f = e^{x_1}4x_1^2 + 2x_2^2 + 4x_1x_2 + 2x_2 + 1 \quad (2.53)$$

The initial point is taken as $x_o = [-1, 1]$ for TRM. The optimum value found is put forth by employing both genetic algorithm (GA) and trust region method (TRM). The table 2.3 shows a detailed comparison of both techniques. Also the figure 2.2 visually aid us by presenting the results of both algorithms. Genetic algorithm can be visualized through best fitness plot that provides best and mean function value through each iteration and best individual plot to show vector entries of the best individual through each generation , whereas the results of trust region method are shown by current point plot that demonstrates the point value at current iteration and function value plot that gives the best function value at each iteration.

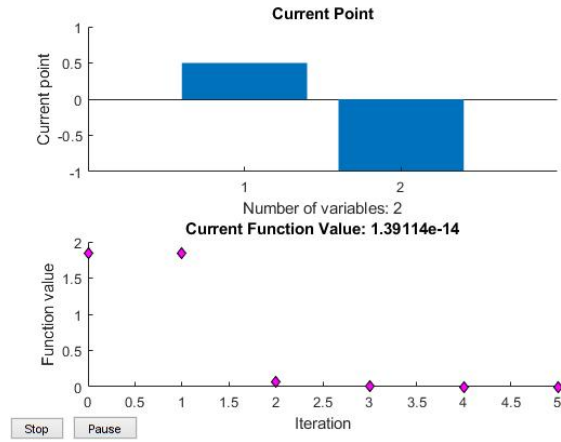
Table 2.3: A comparison of Trust Region Method and Genetic Algorithm with tolerance e^{-6}

Method	optimum function value	x		number of iterations	Optimum	function count
		x_1	x_2			
GA	1.260057884924656e-298	-700.328	70.541	51	global	2600
TRM	1.3911e-14	0.5	-1	5	local	6

It can be observed from the table 2.3 and visualized through the figure 2.2 that although TRM has a accelerated convergence but it failed to reach global minimum for a very simple problem instead it converged to a local optimum point. Whereas although GA consumes a lot of time but it is more reliable and converges to global optimum most of the time. Also TRM requires an initial point and gradient function to be provided whereas genetic algorithm makes no such demands. Hence it can be concluded that genetic algorithm is more appropriate choice for our problem which is a lot more complex than the above presented problem.



(a)



(b)

Figure 2.2: (a):GA-best fitness and best individual plot (b):TRM-current point and function value plot

Chapter 3

Optimal Configuration of an Annular Sector Duct

3.1 Introduction

Optimization is immensely significant in the study of computational fluid mechanics. In this chapter we will optimize fluid flow and heat transfer through the computational domain that was examined in the preceding chapter. Results will be evaluated for the product of fanning friction factor to Reynolds number (fRe) and Nusselt number (Nu). Their response to the alterations in ratio of radii, permeability and number of fins will be analyzed. Also optimized geometries for different permeabilities will be observed.

The mathematical problem is essentially the same as discussed in chapter 2 and it is modeled with the same boundary conditions.

3.2 Optimization Problem

For current research, optimization of a finned annulus is carried out which is created by concentric pipes, with constraints on the physical attributes of the duct. The ratio of radii ($\tilde{R} = \frac{r_i}{r_o}$) and number of fins (nof) are bounded to provide us a better understanding of

the behavior of objective function. The Colburn's j factor is maximized for ratio of radii and sector angle of channel. Colburn's j factor is a non-dimensional quantity which is an analogy that relates heat transfer coefficients, mass transfer coefficients and friction factor.

The significance of this research can be highlighted through the figures 3.2 and 3.1. In the figures 3.2 and 3.1, we demonstrate the effect of \tilde{R} on Nu and fRe respectively for a given value of permeability. These figures express a general trend for distinct values of \tilde{R} . Here the value of permeability is kept constant at 0.001 i.e $\hat{K} = 0.001$. It is observed in figure 3.1 that with the increase in nof , fRe experiences a downward slope for all values of \tilde{R} . Also it can be observed that with the increase in the value of \tilde{R} , the passage for fluid flow decreases hence the curve that shows the trend of fRe starts straightening out, the peak values of graph decreases but a general increase in the value of fRe is observed, this happens due to the constriction in space which restricts the motion of fluid hence causing friction effect to increase. Now through figure 3.2 it could be observed that when \tilde{R} is small, in the beginning (for smaller values of nof) Nu increases then gradually starts decreasing (for larger values of nof) whereas with the increasing value of \tilde{R} the trend is reversed. This non-monotonic behavior is an indication of an optimal geometry for which heat transfer rate can be maximized. The detail on the behavior of fRe and Nu to that of nof can be observed in [21].

Hence our aim is to find an optimum solution for which heat transfer rate is maximum whereas friction effect is at its minimum. We can visualize the behavior of Nu and fRe for a handful of values of \tilde{R} by taking 0.1 increment between adjacent values of \tilde{R} through the figures 3.2 and 3.1, which represent the results for only eight values of \tilde{R} against $\hat{K} = 0.001$. Now if we take full range of parameters i.e $nof = [2:24]$ hence $\alpha \in [0.1309 \ 1.5707]$ and $\tilde{R} \in [0.1 \ 0.75]$ this would generate an infinite number of choices hence searching for an optimum value where j factor is maximum seems to be a gigantic task. Therefore this necessitates the usage of a numerical optimization technique hence genetic algorithm is employed which searches for the optimum through all the available choices.

Our objective is to maximize the heat transfer rate and minimize the friction effect simultaneously, which can prove to be a difficult task. This can be achieved with the help of Colburn's j factor quite easily, which is a correlation between the Nusselt number (Nu) and the product of fanning friction and Reynold's number (fRe). Genetic algorithm maximizes the value of j factor. Hence through Colburn's j factor Nu is being maximized and fRe minimized simultaneously, this solves our problem of choosing the best desirable result perfectly.

3.2.1 Modeling of Genetic Algorithm

Genetic algorithm is employed for finding the best possible results under the assumptions taken for fluid flow and heat transfer as stated above. Also the computational domain remains consistent as mentioned earlier.

Objective Function

The objective function or fitness function for genetic algorithm is taken as the inverse of Colburn's j factor, which is minimized for ratio of radii and sector angle of channel. Hence by maximizing the j factor we increase the convective heat transfer rate and minimize the friction effect.

Constraints

The prime parameters i.e ratio of radii \tilde{R} and the sector angle α (which is shown with the help of number of fins (nof))are bounded by the restrains on their range. For the present optimization process, the range on parameters are taken to be $nof = [2:24]$ hence $\alpha \in [0.1309 \ 1.5707]$ and $\tilde{R} \in [0.1 \ 0.75]$.

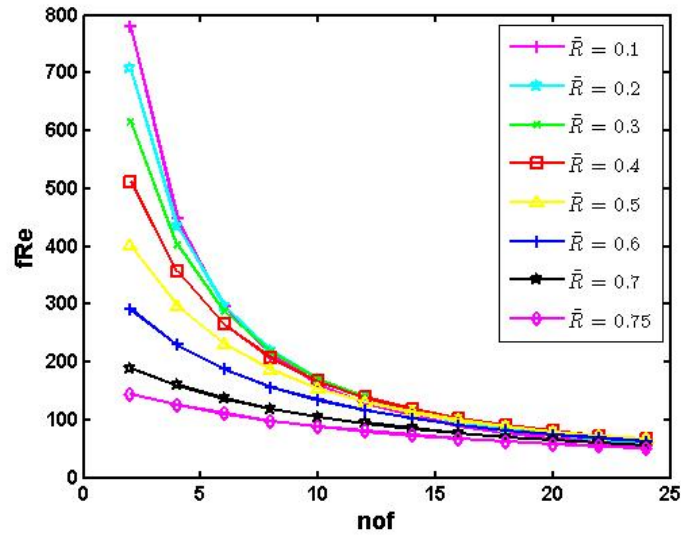


Figure 3.1: Values of fRe for various \tilde{R}

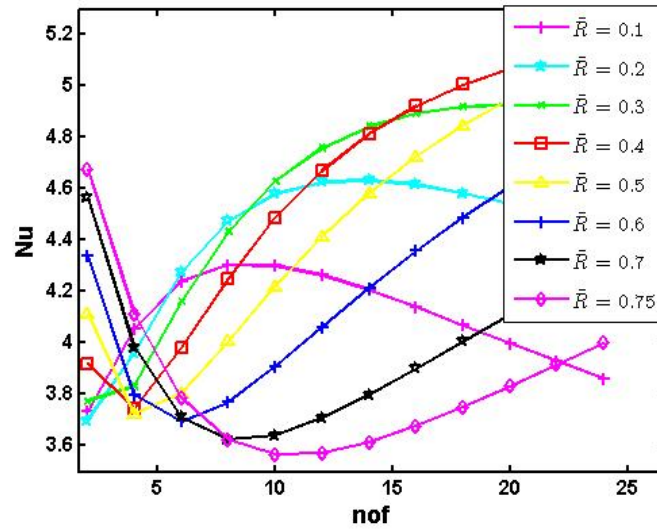


Figure 3.2: Values of Nu for for various \tilde{R}

Penalty Functions

Genetic algorithms can be directly applied to unconstrained problems. If the need arises to apply GA on constrained problems then the most commonly used method to handle constraints is penalty function. Penalty function transforms constrained problems to

unconstrained problems and then solves them. For more information on penalty function refer to [33].

3.3 Results and Discussion

In this section we will be discussing the results of fluid flow and heat transfer for optimal geometries at Prandtl number 0.707, which is Pr for air. Also a comparison has been made for objective function value when Pr is set to be 7.01, which is Pr for water.

The results of Genetic algorithm, when Prandtl number is fixed at 0.707 and permeability i.e $\hat{K} \in [0.001 \ 100]$ can be visualized through figures 3.3 and 3.4 . The figure 3.3 is the graphical representation of the best and mean scores of penalty function, through each generation. As our number of fins are bound to be integers and our optimization lies in the category of constrained optimization hence genetic algorithm minimizes penalty function instead of fitness function. The figure 3.3 exhibit the behavior of inverse of j factor i.e. $\frac{1}{jfactor}$ by its best and mean values versus generations. It can be seen, in an individual plot, that in the initial generations the best and mean penalty values are far apart but rapidly the maximum value declines and comes almost in line with the mean score values until the algorithm converges, the stopping criteria is met and generations of objective function stop. This shows that genetic algorithm is working by decreasing the value of fitness function through each generation. Also as the permeability of porous medium, \hat{K} increases shown in figure 3.3(a)-3.3(f) the best penalty value decreases. This occurs due to the more available space for fluid flow hence friction effect and convective heat transfer decrease but the decrease in friction is more prominent than heat transfer hence this results in a decline in the objective function value.

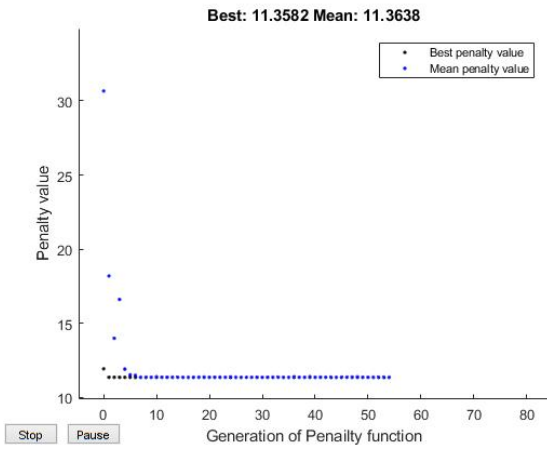
The figure 3.4 portrays the minimum, maximum and the average values of fitness function in each generation, it is recognized as the range plot. The sub-figures (3.4 a)-(3.4 f) describe effect of permeability \hat{K} on the fitness function through generations. It can be observed that best, worst and mean scores of objective function come close to

each other with each passing generation as genetic algorithm converges. Similar to the phenomena that was observed in Best Fitness Plot, it can be seen through each sub-figure in figure 3.4 that with the increases in \hat{K} the over all objective function value decelerates. Also with the rising value of \hat{K} the free available space for fluid flow increases hence the friction effect represented by fRe and heat transfer recognized through Nu decreases but the decrease in fRe is greater than Nu so objective function experiences a decrease in its value.

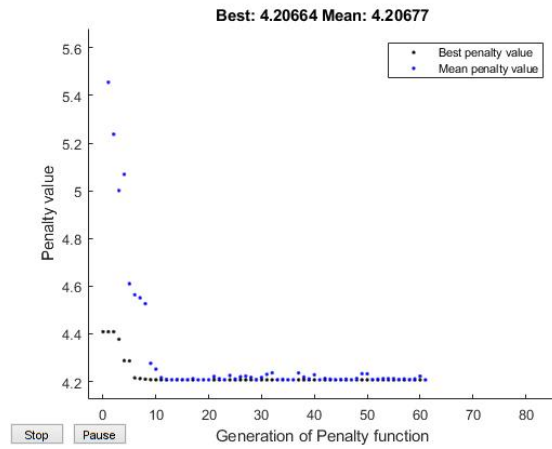
Table 3.1 demonstrates the influence of permeability on the optimum geometry exhibited by geometric components such as ratio of radii \tilde{R} and number of fins (nof) where the Prandtl number is fixed to be 0.707. The corresponding optimum values of Nu and fRe are also given for each value of permeability in porous media, along with the maximum value of objective function (j factor). Where nof is bounded as: $nof = [2 : 24]$, $\alpha \in [0.1309 \ 1.5707]$ and $\tilde{R} \in [0.1 \ 0.75]$. The table shows that with the decrease in permeability of porous media the value of objective function gradually declines, whereas fRe and Nu increases but the upsurge in fRe is more notable than the increase in Nu . As j factor is a correlation between Nu and fRe then this behavior of Nu and fRe decreases the value of j factor. The changes in fRe and Nu arises due to the high dependence of friction factor and Nusselt number on the conduct of ratio of radii, number of fins and permeability.

It can be observed that with the decrease in \hat{K} , the optimum or best value of \tilde{R} experiences a slow decrease in its value whereas nof is constant at maximum value of fins. So due to less free space, as both \tilde{R} and permeability of porous media are small fRe becomes large but it is still the least, most feasible amount for a particular value of permeability. Nu experiences slight fluctuations which are very minuscule but on the whole it increases. This slight elevation in the value of Nu can be due to porous media, as permeability decreases the porous media becomes more packed hence helps increase the rate of heat conduction. The optimum value of number of fins is seen to be at its maximum value because as the fins are taken to be highly conductive then greater the

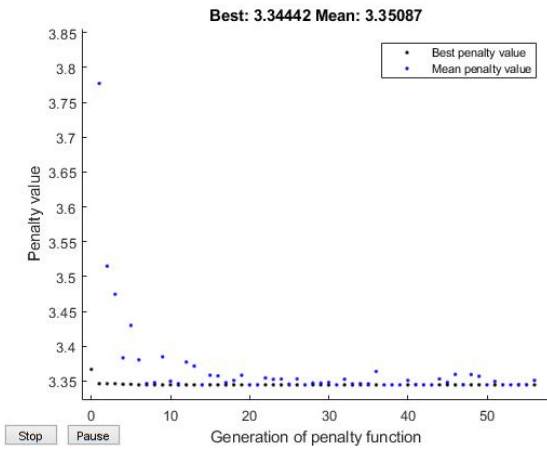
amount of heat conducting surface more will be the rate of convective heat transfer. With the decreases in \hat{K} , the optimum value of \tilde{R} experiences a minute decreases hence more space is available for fluid flow which creates a balance with the low permeability, so that the desired surge in Nu is achieved.



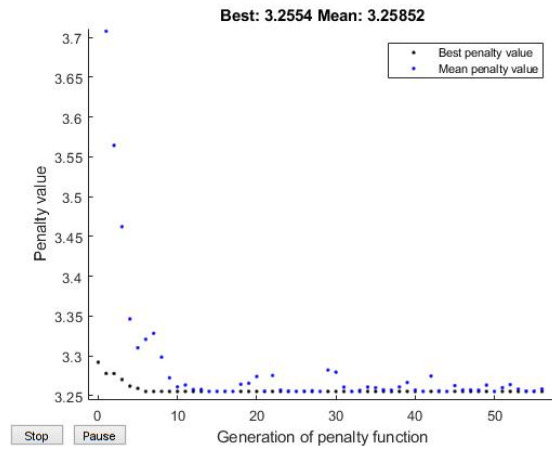
(a)



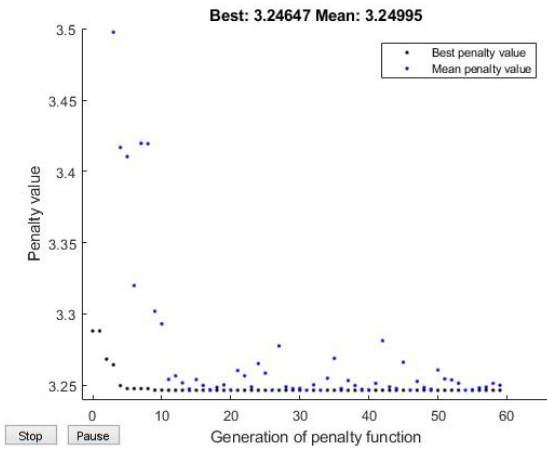
(b)



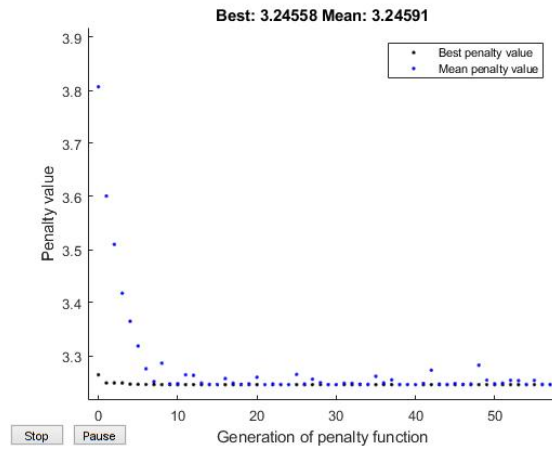
(c)



(d)

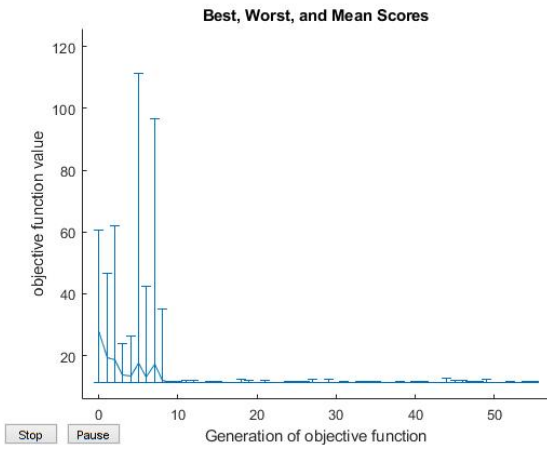


(e)

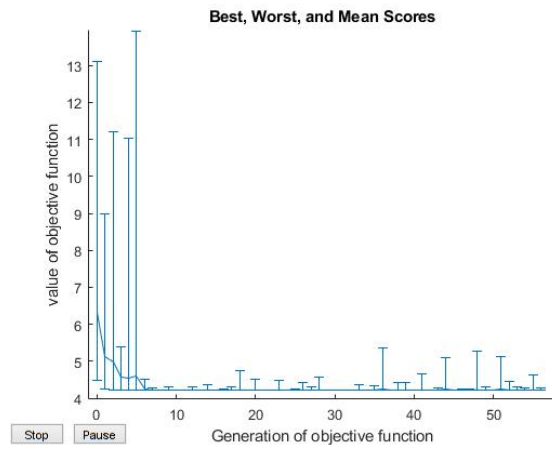


(f)

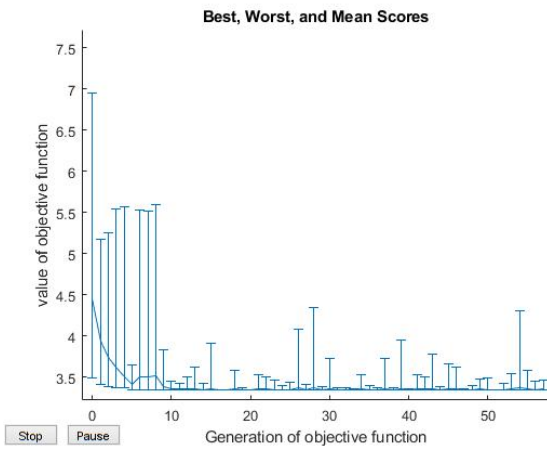
Figure 3.3: Best fitness plot at $Pr=0.707$ for (a): $\hat{K} = 0.001$ (b): $\hat{K} = 0.01$ (c): $\hat{K} = 0.1$ (d): $\hat{K} = 1$ (e): $\hat{K} = 10$ (f): $\hat{K} = 100$



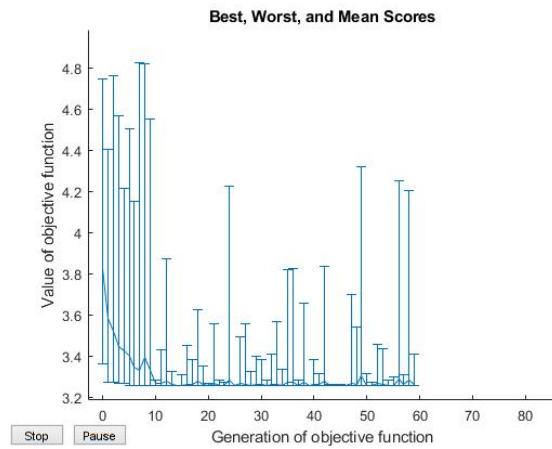
(a)



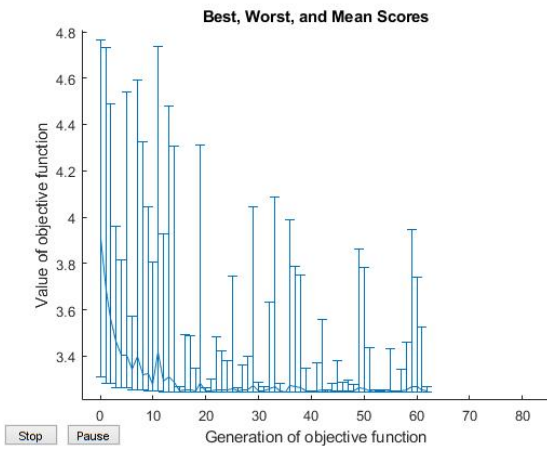
(b)



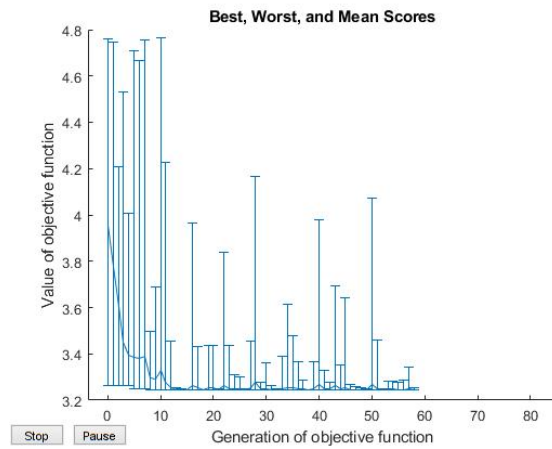
(c)



(d)



(e)



(f)

Figure 3.4: Range plot at $Pr = 0.707$ when (a): $\hat{K} = 0.001$ (b): $\hat{K} = 0.01$ (c): $\hat{K} = 0.1$ (d): $\hat{K} = 1$ (e): $\hat{K} = 10$ (f): $\hat{K} = 100$

It is noted that optimal value of ratio of radii \tilde{R} at each value of \hat{K} , is found almost midway in the range set for \tilde{R} i.e $\tilde{R} \in [0.1 \ 0.75]$. This behavior indicates that optimum value does not occur when \tilde{R} at its maximum because for large values of \tilde{R} , fRe raises (due to less available space for fluid flow) which is not our desired outcome. Genetic algorithm looks past the smaller values in range of \tilde{R} for optimum because although friction effect decreases so does the convective heat transfer rate due to large distance between heated surfaces. Hence a middle value gives optimum.

Table 3.1: Effect of permeability on geometric parameters

\hat{K}	Geometric Components		j factor	fRe	Nu
	\tilde{R}	nof			
100	0.570127758897386	24	0.308111604235642	15.605687585626500	4.283486819490765
10	0.570115335784497	24	0.308026794022231	15.610494379960882	4.283626772414494
1	0.569991181369073	24	0.307181547770969	15.658558525894634	4.285025151868879
0.1	0.568709076515744	24	0.299005429710323	16.139216984288254	4.299005558385511
0.01	0.553392324178606	24	0.237719484798629	20.944235305204661	4.435430311389410
0.001	0.416706766714202	24	0.088042418303868	65.787935927488192	5.159940515716588

We exhibit in the table 3.2, the impact of two different permeabilities on optimum duct geometry where a comparison is done for the value of Prandtl number taken to be 7.01, which is Pr for water at 20 degree centigrade and $Pr= 0.707$. The table shows that, with the decrease in permeability of porous media, for both values of Prandtl number, j factor shows a steady decline. This occurs due to the co-dependence of j factor on fRe and Nu . fRe and Nu increases with the decrease in \hat{K} but the upsurge in fRe is more notable than the increase in Nu . The value of j factor for $Pr= 0.707$ is more then that of $Pr= 7.01$ at every \hat{K} ; because when Pr is small, thermal diffusivity is more than kinematic viscosity means thermal boundary layer increases so there is a faster heat transfer rate,

whereas for larger values of Pr velocity boundary layer shows an upsurge but that can be at the cost of an increase in friction effect (refer to definition of Prandtl number 1.3.7). So to increase heat transfer rate Pr should be kept small; hence at $Pr=0.707$, j factor shows greater values than $Pr=7.01$ as j factor is ratio of Nu to the product of fRe and a power of Pr . The optimum \tilde{R} show a decreasing trend with the decrease in \hat{K} and it is same for both the values of Pr up-till the eighth decimal place. As our aim was to maximize j factor hence a smaller value of Pr is more preferable for greater heat transfer and the reduction of friction effect. The optimum nof occur in a constant manner at its maximum range value, for the two Pr , due to the high conductivity of heat transferring surface of fins. Hence optimum duct geometry, at which we get maximum heat transfer and minimum friction effect shows a slight difference for both values of Pr at each \hat{K} .

Table 3.2: A comparison of optimum geometric parameters between $Pr = 0.707$ and $Pr = 7.01$

\hat{K}	$Pr=0.707$			$Pr=7.01$		
	j factor	\tilde{R}	nof	j factor	\tilde{R}	nof
100	0.308111	0.570127759	24	0.143420	0.570127761	24
10	0.308027	0.570115335	24	0.143380	0.570115374	24
1	0.307181	0.569991181	24	0.142987	0.569991177	24
0.1	0.299005	0.568709076	24	0.139181	0.568709079	24
0.01	0.237719	0.553392324	24	0.110653	0.553392317	24
0.001	0.088042	0.416706767	24	0.040982	0.416706732	24

Now the impact created by various permeabilities over the optimum velocity profile would be analyzed, where $\hat{K} \in [0.001 \ 100]$. The figure 3.5 show the velocity contours for the optimal value of \tilde{R} and α . After examining the sub-figures (3.5 a) to (3.5 f) an increase in the velocity gradients among adjacent layers in the fluid as \hat{K} declines can be observed. This is the reason behind the decrease in bulk velocity and increases the

fRe with decreasing permeability. As the permeability falls the maximum velocity region grows.

Figures 3.6 exhibit the isotherms for optimal value of \tilde{R} and α , at each \hat{K} . The sub-figures (3.6 (a))-(3.6 (f)) demonstrate the influence created by decreasing the permeability on the temperature profile. Through the impressions of sub-figures a temperature difference from the heated surfaces can be observed, heated surfaces being the wall of inner pipe and the fin surface. Through the sub-figures (3.6 (a))-(3.6 (f)) it can be detected that, with the decline in permeability heat transfer increases gradually as the temperature variance among heated surface and the fluid flowing over it grows at a particular point.

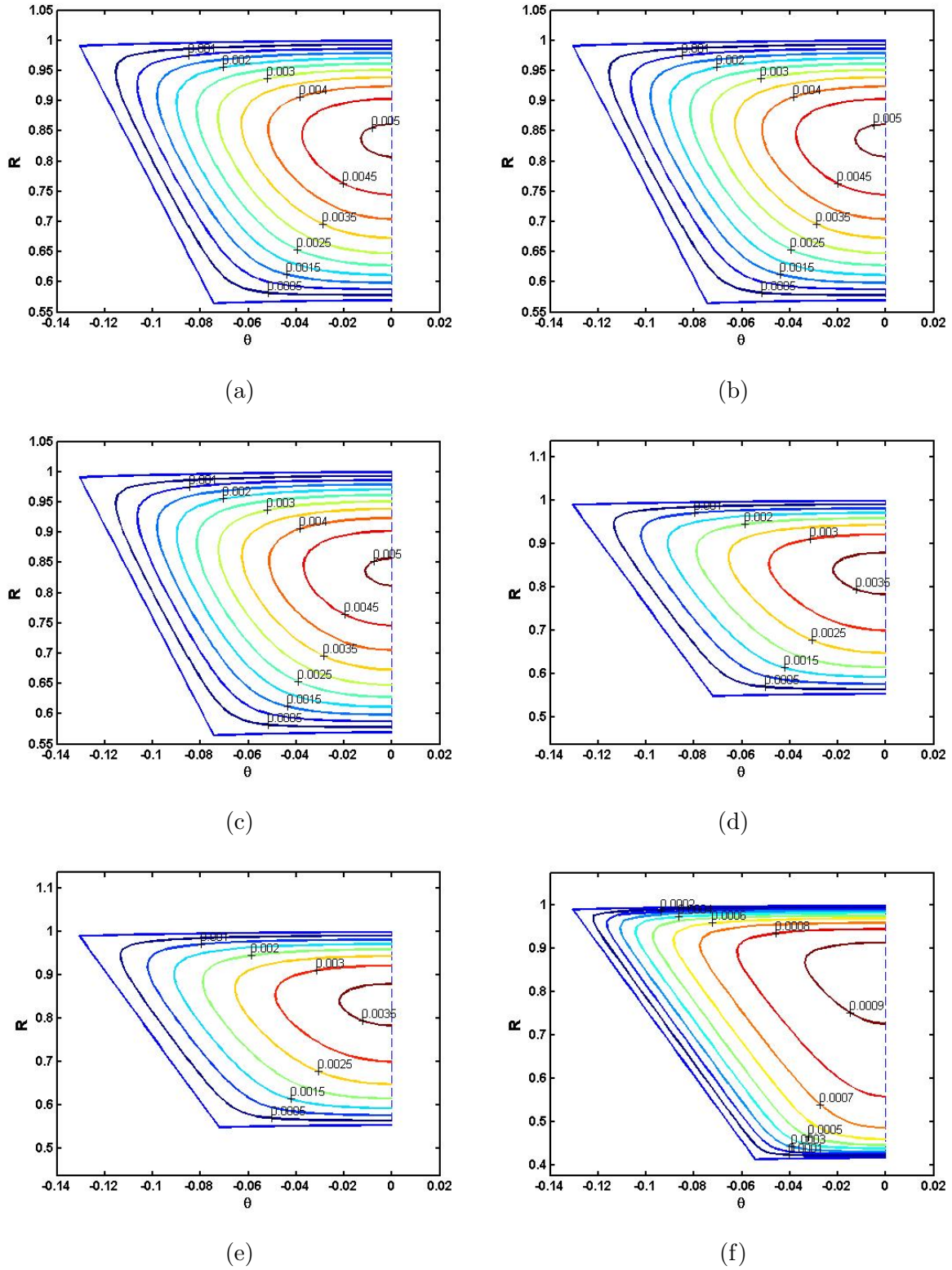
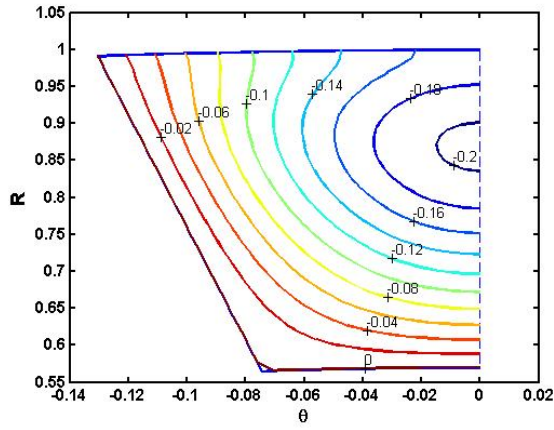
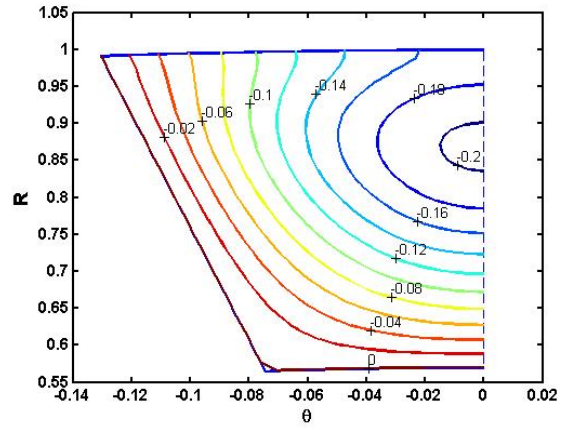


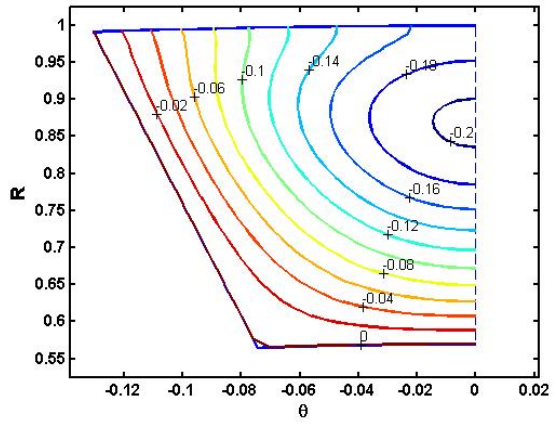
Figure 3.5: Velocity profile at $Pr=0.707$ for (a): $\hat{K} = 100$ (b): $\hat{K} = 10$ (c): $\hat{K} = 1$ (d): $\hat{K} = 0.1$ (e): $\hat{K} = 0.01$ (f): $\hat{K} = 0.001$



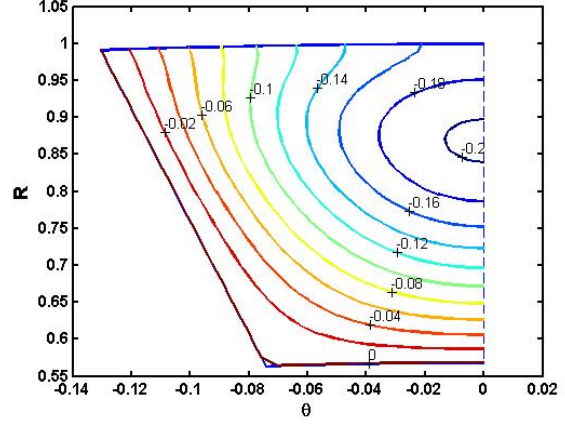
(a)



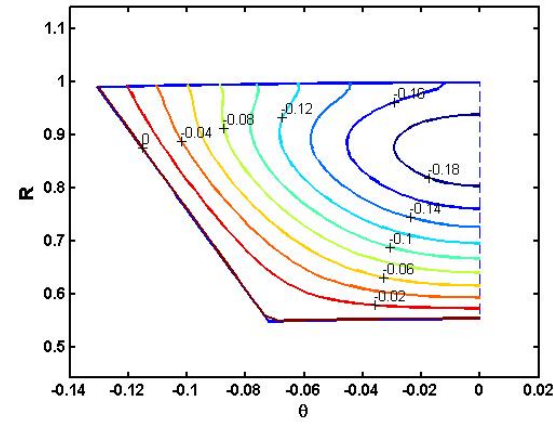
(b)



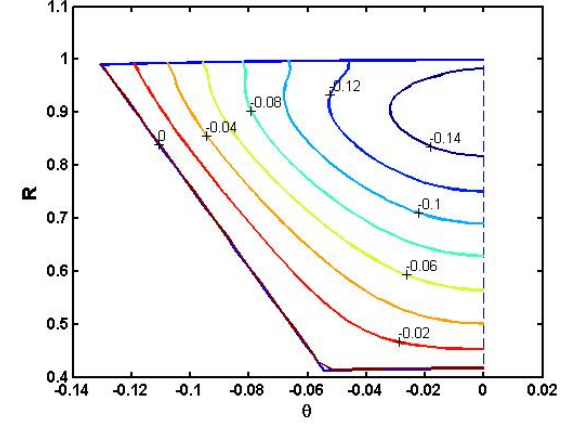
(c)



(d)



(e)



(f)

Figure 3.6: Temperature profile at $Pr=0.707$ for (a): $\hat{K} = 100$ (b): $\hat{K} = 10$ (c): $\hat{K} = 1$ (d): $\hat{K} = 0.1$ (e): $\hat{K} = 0.01$ (f): $\hat{K} = 0.001$

Chapter 4

Conclusions and Further work

In this research, the optimization of an annulus sector duct filled with Darcy-Brinkman's porous media has been conducted. We have optimized ratio of radii and number of fins by employing genetic algorithm (GA) while considering j factor as our objective function. The problem is subjected to H_1 boundary condition, executed at the insides of heat conducting surfaces. Where all the heat transferring surfaces in the duct are considered isothermal. A comparison has been conducted for objective function at Prandth number 0.707 and 7.01. Also the influence of various permeabilities on optimal geometries was analyzed.

4.1 Conclusions

The following results can be summarized from the study conducted above

- With the decrease in permeability, the optimum values of fRe and Nu both exhibit an increase.
- The optimal number of fins is at its upper bound value and it remains consistent for all values of permeabilities.
- The optimum j factor decreases with the decrease in permeability due to the increase

in values of fRe and Nu but the upsurge in fRe is more prominent than Nu .

4.2 Further extensions

Furthermore this study opens doors to extend this work in various directions. Some of them are given as under

- For this research, we have taken the fins to be fully conductive but other conduction effects, such as conjugate approach, through the longitudinal fins can be considered.
- Geometric parameters such as height, thickness and shape of fins can be altered.
- In current study, we have only considered limited cases for Prandtl number, considering water and air at certain temperatures. Hence the value of Prandtl number can be manipulated.
- A dimensionless environment is considered for present study which can be changed.

References

- [1] H. Hareem, M. Iqbal, *Optimal configuration of an annular sector duct filled with porous media*. Communications in Mathematics and Application, submitted.
- [2] F. Liu, *The effect of geometries on heat transfer enhancement of thermal fluids in curved ducts*. Applied Thermal Engineering, 90 (2015), 590–595.
- [3] I. Kurtbas, N. Celik, *Experimental investigation of forced and mixed convection heat transfer in a foam filled horizontal rectangular channel*, International Journal of Heat and Mass Transfer, 52 (2009), 1313–1325.
- [4] K. Hooman, H. Gurgenci, A. A. Merrikh, *Heat transfer and entropy generation optimization of forced convection in porous-saturated ducts of rectangular cross-section*, International Journal of Heat and Mass Transfer, 50 (2007), 2051–2059.
- [5] M. R. H. Nobari, M. T. Mehrabani, *A numerical study of fluid flow and heat transfer in eccentric curved annuli*, International Journal of Thermal Sciences 49 (2010), 380–396.
- [6] Z. Y. Li, T. C. Hung, W. Q. Tao, *Numerical simulation of fully developed turbulent flow and heat transfer in annular-sector ducts*, Heat and Mass Transfer, 38(4-5) (2002), 369-377.
- [7] E. H. Zaim and S. A. G. Nassab, *Numerical investigation of laminar forced convection of water upwards in a narrow annulus at supercritical pressure*, Energy, 35(10) (2010), 4172–4177.

- [8] O. Zeitoun, A. S. Hegazy, *Heat transfer for laminar flow in internally finned pipes with different fin heights and uniform wall temperature*, Heat Mass Transfer 40 (2004) 253-259.
- [9] M. J. Lin, Q. W. Wang, W. Q. Tao, *Developing Laminar Flow and Heat Transfer in Annular-Sector Ducts*, Heat Transfer Engineering 21(2) (2000) 53–61.
- [10] I. K. Adegun, T. S. Jolayemi , O. A. Olayemi , A. M. Adebisi. *numerical simulation of forced convection heat transfer in inclined elliptical ducts with multiple internal longitudinal fins*. Alexandria Eng. J. (2017).
- [11] M. Kaviani, *Laminar flow through a porous channel bounded by isothermal parallel plates*, International Journal Heat Mass Transfer, 28(4) (1985), 851–858.
- [12] M. Ishaq, K. S. Syed, Z. Iqbal, A. Hassan, A. Ali, *DG-FEM based simulation of laminar convection in an annulus with triangular fins of different heights*, International Journal of Thermal Sciences 72 (2013), 125–146.
- [13] O. Cekmer, M. Mobedi, B. Ozerdem , I. Pop, *Fully developed forced convection heat transfer in a porous channel with asymmetric heat flux boundary conditions*, Transport in Porous Media 90(3) (2011) 791.
- [14] H. J. Sung, S. Y. Kim, J. M. Hyun, *Forced convection from an isolated heat source in a channel with porous medium*, International Journal Heat and Fluid Flow, 16 (1995), 527–535.
- [15] S. Colle, C. R. Maliska, *Optimization of finned double tubes for heat transfer in laminar flow*, Brazilian Congress on Mechanical Engineering, vol. B. Rio de Janeiro, Universidade Federal, (1976), 475-490.
- [16] G. Fabbri, *A genetic algorithm for fin profile optimization*, International Journal of Heat and Mass Transfer, 40 (9) (1997), 2165–2172.

- [17] Z. Iqbal , K. S. Syed and M. Ishaq, *Optimal fin shape in finned double pipe with fully developed laminar flow*, Applied Thermal Engineering 51 (2013), 1202–1223.
- [18] Z. Iqbal , K. S. Syed, M. Ishaq, *Optimal configuration of finned annulus in a double pipe with fully developed laminar flow*, Applied Thermal Engineering, 31 (2011), 1435–1446.
- [19] Z. Iqbal, K. S. Syed, M. Ishaq, *Optimal convective heat transfer in double pipe with parabolic fins*, International Journal of Heat and Mass Transfer, 54 (2011), 5415-5426.
- [20] Z. iqbal, K. S. Syed, M. Ishaq, *Fin design for conjugate heat transfer optimization in double pipe*, International Journal of Thermal Sciences, 94 (2015), 242–258.
- [21] M. Iqbal, H. Afaq, *Fluid flow and heat transfer through an annular sector duct filled with porous media*, Journal of porous media, 18(7) (2015), 679–687.
- [22] B. R. Munson, D. F. Young, T. H. Okiishi, W. W. Huebsch, *Fundamentals of Fluid Mechanics*, J. Wiley and Sons, 6 (2009).
- [23] R. W. Fox, A. T. McDonald, P. J. Pritchard, *Introduction to Fluid Mechanics*, J. Wiley and Sons, 6 (2009).
- [24] F. P. Incropera, D. P. DeWitt, T. Bergman, A. Lavine, *Fundamentals of Heat and Mass Transfer*, J. Wiley, 6 (2007).
- [25] Jr. J. D. Anderson, *Computational Fluid Dynamics*. McGraw Hill, 1 (1995).
- [26] H. K. Versteeg, W. Malalasekera *An introduction to computational fluid dynamics: The finite volume method*. Longman scientific and technical, 2 (1995).
- [27] S. Kakaç, Y. Yener *Convective Heat Transfer*. CRC press, 2 (1995).
- [28] R. K. Shah and A. L. London, *Laminar Flow Forced Convection in Ducts*, Academic Press, London, 1 (1978).

- [29] S. Gosselin, *Review of utilization of genetic algorithms in heat transfer problems*, International Journal of Heat and Mass Transfer 52 (2009), 2169–2188.
- [30] A. R. Conn, N. I. M. Gould, Ph. L. Toint, *Trust-Region Methods*, MPS-SIAM Series on Optimization. SIAM, Philadelphia (2000).
- [31] Y. X. Yauan, *A review of trust region algorithms for optimization*. J.M. Ball, J.C.R. Hunt (Eds.), Proceedings of the Fourth International Congress on Industrial and Applied Mathematics, Oxford University Press, (2000), 271–282.
- [32] B. Wallace, *Constrained optimization: Kuhn-Tucker conditions* Economics dept, (2004).
- [33] Ö. Yeniay, *Penalty function methods for constrained optimization with genetic algorithms* Mathematical and Computational Applications, 10(1) (2005), 45–56.
- [34] Geankoplis, *C.J. Transport processes and separation process principles*, 4 (2003), 475.